Development of a DNA transfer technique for human lung cells with synthetic peptide Tat-RGD and its application for regulatory and functional analysis of RELMβ

Inauguraldissertation

zur Erlangung des Grades eines Doktors der Humanbiologie

des Fachbereichs Medizin

der Justus-Liebig-Universität Gießen

Vorgelegt von

Aparna Renigunta

aus Hyderabad, India

Giessen 2005

Aus dem Zentrum für Innere Medizin, Medizinische Klinik II

Direktor: Prof. Dr. med. Werner Seeger

Des Universitätsklinikums Giessen und Marburg

Gutachter : Priv.-Doz. Dr. rer. nat. Jörg Hänze

Gutachter: Priv.-Doz. Dr. med. Ludger Fink

Tag der Disputation : 17. 05. 2006

నా ఈ పరిశోధనా గ్రంథాన్ని
తాతయ్య కుడుము గోవిందు గారికి,
ప్రియమైన అమ్మ నాన్నకు
అంకితం చేస్తున్నాను.

రేణిగుంట అపర్ణ

Index

Index

List of Figures

List of tables

Abbreviations

Index

List of figures:

.

List of tables:

Abbreviations:

AA	Amino acid
AP	Alkaline phosphatase
APS	Ammonium persulfate
BSA	Bovine serum albumin
bp	Base pair
cDNA	Complementary deoxyribonucleic acid
CMV	Cyto megalie virus
Da	Dalton
DL	DNA- Lipofectamine complex
dNTP	deoxyribose nucleotide triphosphate
ddNTP	di-deoxyribose nucleotide triphosphate
DMSO	Dimethylsulfoxide
DOPE	Dioleoylphosphatidyl ethanolamine
DOTAP	1, 2-diacyl-3-trimethylammonium propane
DOTMA	[2, 3-bis(oleoyl)propyl]-trimethyl]ammoniumchloride;
ds	Double strand
DTT	Dithiothreitol
ECL	Enhanced chemiluminescence
EDTA	Ethylendinitrilo-N,N,N',N',-tetra-acetate
FCS	Fetal calf serum
FIZZ	Found in inflammatory zone
GFP	Green fluorescence protein
Hepes	2-(-4-2-hydroxyethyl)-piperazinyl-1-ethansulfonate
HIMF	Hypoxia-induced mitogenic factor
HIV1	Human immuno deficiency virus type-1
HRP	Horseradish peroxidase
kb	Kilo base
kDa	Kilo Dalton
LB	Luria Bertani

Abbreviations

LMW	Low molecular weight
Luc	Luciferase
mV	milli volts
MW	Molecular weight
NaCl	Sodium chloride
NaOH	Sodium hydroxide
NLS	Nuclear localization signal
nm	Nano meters
OD	Optical density
PCR	Polymerase Chain Reaction
PEG	Poly-ethylene glycol
PEI	Poly-ethylene imine
PLL	Poly-*L*-lysine
R/ (Arg)	Arginine
RGD	Tri-peptide sequence containing arginine, guanine, aspartic acid
RNAi	Ribonucleic acid inhibitor
RNase	Ribonuclease
Rpm	Revolutions per minute
RT	Room temperature
SDS	Sodium dodecyl sulfate
ss	Single strand
TAE	Tris acetate EDTA buffer
TAR	Transactivation response
Tat	Transactivator protein
TEMED	N',N',N',N'-Tetra methyl diamine
TRD	TatRGD/ DNA complex
TRDL	TatRGD/ DNA/ Lipofectamine complex
Tris	Tris-(hydroxy methyl)-amino methane
UV	Ultra violet

1. Introduction:

1.1 Non-viral gene transfer:

Altering or manipulating genes or gene expression has tremendous therapeutic potential for the treatment of a variety of inherited or acquired disorders. Gene therapy aims at treating diseases by delivering DNA, RNA, antisense or RNAi (double stranded RNA) sequences that alter gene expression within a specific cell population, thereby manipulating cellular processes and responses. Recent advances in molecular biology combined with the culmination of the Human Genome Project have provided a genetic understanding of cellular processes and disease pathogenesis (**1**). Numerous genes involved in disease and cellular processes have been identified as targets for therapeutic approaches. However, the development of novel therapeutic strategies using these targets is dependent on the ability to manipulate the expression of these target genes in the desired cell population.

Gene therapy can manipulate gene expression either *in vitro* or *in vivo*. The *in vitro* approach involves genetically modifying cells, which are isolated either from the patient or from a donor, that are subsequently implanted into the patient (**2).** The challenge of gene therapy is to develop safe and efficient gene-delivery systems. Viral vectors generally provide the most efficient gene transfer. The premise of viral gene delivery is to use viruses that have sections of their genome removed to make them replication deficient. Within the section that was removed, genes encoding for therapeutic proteins can be inserted. Viruses are produced using helper cell lines that create attenuated viruses that can efficiently deliver the therapeutic gene but are incapable of replicating *in vivo*. The limited space to insert genes into the viral genome combined with issues associated with virus production and safety has inspired the development of non-viral DNA delivery systems. Non-viral approaches typically involve plasmids (circular DNA), Oligonucleotides (short single stranded DNA or RNA) or RNAi. Plasmid DNA, Oligonucleotides and RNAi are generally considered to be safe; however, the gene transfer efficiency is significantly less than viral vectors and must be improved for many therapeutic applications (**3**).

1.2 Barriers against effective gene delivery:

Effective gene delivery requires; that the plasmids, oligonucleotides or RNAi that is to be delivered to the desired cell population is efficiently internalized by the cell and transported to the appropriate cellular compartment. Though the path is known, many barriers exist which limit the efficiency of delivery. Endonucleases present in the extra-cellular space can degrade non-viral DNA within 30 minutes (**4**). The inability to cross biological membranes, such as the plasma membrane, and the nuclear membrane is due to the size and charge density of naked DNA.

Plasmid DNA is typically 10^3 to 10^4 base pairs in length, has a super-coiled tertiary structure in aqueous solution, a molecular weight of 10^6 to 10^7 Daltons, and an effective hydrodynamic diameter greater than 100 nm (**5**). The surface charge density of naked DNA, which has zeta potentials ranging from -30 mV to -70 mV, creates repulsion between the DNA and the negatively charged cell surface. This large size and negative surface charge density most likely limits the uptake of DNA by the cells. Delivery systems are being developed to overcome these barriers of stability, size, charge density, and bio-distribution.

1.3 Modes of gene delivery:

Various modes of gene transfer had been designed to enhance gene transfer by improving (i) the stability of DNA, (ii) the efficiency of cellular uptake and the intracellular trafficking or (iii) the bio-distribution of DNA. These modes can be largely divided as Mechanical and Chemical methods of gene delivery.

1.3.1 Mechanical Methods:

Insufficient contact of inherently highly active nucleic acid delivery systems with target cells is a primary reason for their often-observed limited efficacy. Mechanical methods of targeting can overcome this limitation and reduce the risk of undesired side effects due to non-target site delivery (**6).** Physical methods such as Electroporation, Focused laser, Ballistic (gene gun) approaches are known to enhance gene delivery. New generation strategies involving the use of Magnetic field (Magnetofection) have revolutionized the efficiency of non-viral gene transfer. As plasmid DNA appears to be a safe gene vector system, it seems likely that plasmid with physically enhanced delivery will be used increasingly in clinical trials.

1.3.1.1 Electroporation:

Electroporation is a physical process of inducing nanometer-sized transient pores in the cell membrane by the application of short duration, high intensity electric field pulses to cells or tissues. In this permeabilized state, the membrane can allow passage of DNA, enzymes, antibodies and other macromolecules into the cells. The most important parameters for effective electroporation are the voltage [V], the length of time the field is applied (pulse duration), plasmid concentration and electrodes (**7**). Over the last two decades, electroporation equipments have been undergoing considerable refinement. Notably, square wave pulse generators have been constructed. These generators modify the exponential pulse to a square pulse, where pulse amplitude and pulse length can be independently controlled, which is an important pre-requisite for optimization.

Theory of Electroporation:

The transmembrane potential induced in a cell by an external field is generally described by the equation:

$$\Delta V_m = f\, E_{ext}\, r\, \cos\theta$$

Where, **Vm** is the transmembrane potential, f a form factor describing the impact of the cell on the extracellular field distribution, **Eext** the applied electric field, r the cell radius and θ the polar angle with respect to the external field. Many authors list the value for the factor f as **1.5**; however, this factor is dependent on a number of different factors (**8, 9**). Electroporation is achieved when $\Delta V_m > \Delta V_s$ which is the threshold potential. As the bilayer membrane is a common feature for eukaryotic cells, ΔV_s is similar for various cell types. Experimental and theoretical study described ΔV_s as being 200 mV (**10**).

Whereas pore formation happens in the microsecond time frame, membrane resealing happens over a range of minutes with variation depending on the electric parameters used and on temperature. Intact, function of the cytoskeleton is also of considerable importance for pore closure (**11**)

1.3.1.2 Magnetofection:

This method associates DNA with magnetic nano-particles coated with cationic molecules (Magnetofectins). The resulting molecular complexes are then transported into cells supported by an appropriate magnetic field. Magnetofection exploits magnetic force exerted upon gene vectors to drive them towards and possibly even into, the target cells. In this manner, the complete applied vector dose gets concentrated on the cells within a few minutes so that 100% of the cells get in contact with a significant vector dose. High transfection rate achievable with low vector doses and extremely short process time are the major advantages of magnetofection (**12, 13**)

Mechanism involved in the cellular uptake of Magnetofectins:

Magnetofectins are super-paramagnetic iron oxide nano-particles coated with gene carriers like cationic lipids, cationic polymers etc., Magnetofection seems to follow a similar mechanism as found in the cationic gene carrier coating the nano-particles. The presence of the magnetic force leads to a fast accumulation of the complexes on the cell surface but not to a traction of complexes into the cells. Magnetic gene vector complexes are mainly taken into cells by unspecific endocytosis. However, clathrin-dependent and caveoli-mediated uptake, are apparently involved in magnetofection based on the cationic gene carrier coating the nano-particles. The extent of involvement of clathrin-dependent and caveoli-mediated endocytosis is also cell-line-dependent. (**14**)
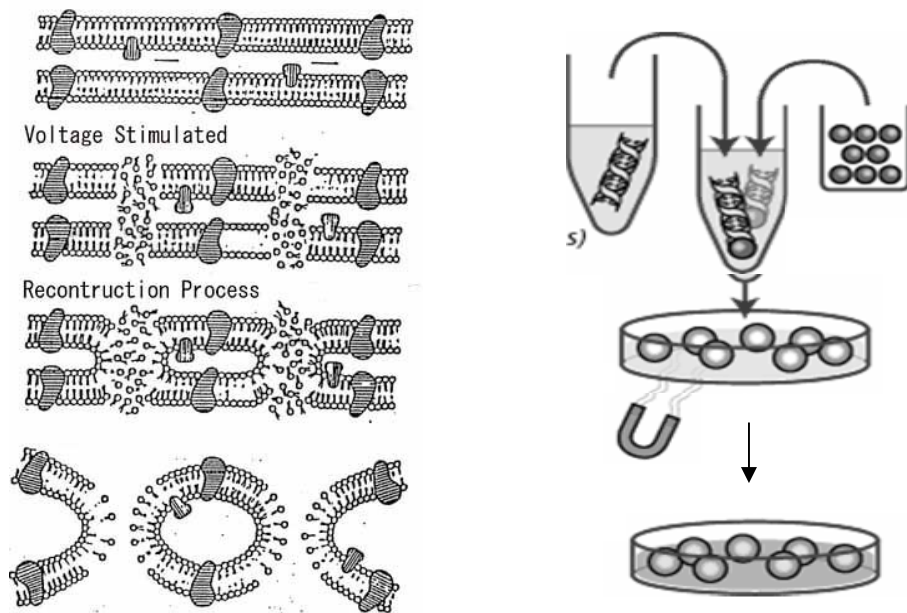
Figure 1: **Electroporation and Magnetofection:** Voltage stimulated transient pore formation during electroporation (left). Application of magnetic field in gene transfer (right).

These mechanical techniques are capable of transfecting cells, possibly by compromising the integrity of the cell membrane thus allowing entry of DNA into the cell. However, the details of the mechanism by which DNA is internalized for the various systems are not well understood **(15)**

1.3.2 Chemical Methods:

These are materials designed to increase gene transfer function to enhance (i) the stability of DNA, (ii) the efficiency of cellular uptake and intracellular trafficking or (iii) the bio-distribution of DNA. The most common approach involves the complexation of naked DNA with cationic lipids or poly (cationic) polymers that package the DNA for effective delivery. This approach typically alters the large negative surface charge on the DNA and facilitates internalization by the cell. These packages can also provide protection against nuclease activity, targeting of a specific cell population, and efficient internalization and intracellular trafficking, all of which can significantly increase gene transfer efficiencies.

1.3.2.1 Cationic Lipids:

The most investigated approach for condensing non-viral DNA for efficient gene transfer is the use of cationic lipids. Felgner and Bennett for oligonucleotides used cationic lipids for the first time to deliver DNA **(16)**. More recently, siRNA has been delivered to mammalian cells using commercially available lipids **(17, 18, 19)**. Although some cationic lipids are used individually to deliver DNA (e.g., DOTAP), many formulations of cationic lipids also contain a zwitterionic or neutral co-lipid, such as DOPE or cholesterol, to enhance transfection. Formulations of cationic lipids have been widely applied for *in vitro* nucleic acid transfection and more than 30 products are commercially available for this purpose, including Lipofectin (a 1:1 mixture of DOTMA and DOPE), Transfectam, Lipofectase, Lipofect-AMINE and LipoTaxi **(20)**.

The main components of a cationic lipid are a hydrophilic lipid anchor, a linker group, and a positively charged head group. The lipid anchor is typically either a fatty acid chain (e.g., derived from oleic or myristic acid) or a cholesterol group, which determines the physical properties of the lipid bi-layer, such as flexibility and the rate of

lipid exchange (**21**). The linker group is an important determinant of the chemical stability, bio-degradability, and transfection efficiency of the cationic lipid. Biodegradable lipids are being developed, which can be metabolized by various enzymes (e.g., esterases, peptidases) to minimize toxicity (**22, 23**). The linker can also provide sites for the introduction of novel side chains to enhance targeting, uptake, and trafficking. The positively charged head group on the cationic lipid self-assembles with the negatively charged DNA and is a critical determinant of the transfection and Cytotoxic properties of liposome formulations. The head groups differ markedly in structure and may be single or multiple charged as primary, secondary, tertiary or quaternary amines. The hydrophobicity of the lipid moiety has a crucial effect on *in vitro* gene transfer. Generally, increase in the linker length corresponds with the increase in gene delivery (**24**).

Mixing of DNA and cationic lipid results in the collapse of DNA to form a condensed structure, termed lipoplex, in which nucleic acids are buried within the lipid. Liposome association with DNA has resulted in tube like bi-layers (**25, 26**), multi-lamellar complexes (**27, 28, 29**), as well as structures containing non bi-layer elements (**30, 31**). These arrangements have demonstrated increased transfection, which is attributed to the relative instability of the complexes due to rapid fusion with anionic vesicles and subsequent DNA release.

The colloidal properties (e.g., size, stability) of the lipoplexes are principally determined by the cationic lipid/DNA charge ratio and not the composition of the lipid or the helper lipid. The charge ratio (+/-) is typically defined as the number of amines on the cationic lipid relative to the number of phosphate groups on the DNA. A neutral charge ratio (1:1 charge ratio for lipid: DNA) is typically avoided because it results in the formation of large aggregates (>1 μm). Lipoplexes prepared at positive charge ratio and negative charge ratio likely represents structures with different lipid and DNA packaging (**32**). At a positive charge ratio, large Multi-lamellar vesicles (LMV, diameter 300 - 700 nm) transfect cells more efficiently (**21, 33, 34**). The order in which DNA and lipid are mixed is critical and significantly affects the lipid and DNA packing (**35, 32**). When adding DNA to lipid, a gradual increase in size was observed. When adding lipid to DNA, the particle size remains roughly constant until the amount of lipid's positive

charge exceeds the nucleic acid's negative charge, whereupon the particles grow rapidly in size (**35**).

The net charge on the lipoplex affects its interactions with other components present *in vivo* and *in vitro* (e.g., media, serum, extra-cellular matrix glycoproteins, mucosal secretions), which can limit the transfection efficiency. A positive charge ratio, which facilitates interactions with the cell membrane, is frequently used for *in vitro* studies (3:1), whereas *in vivo* studies may require the charge ratio to be altered because of interactions with components of the physiological environment (**36**).
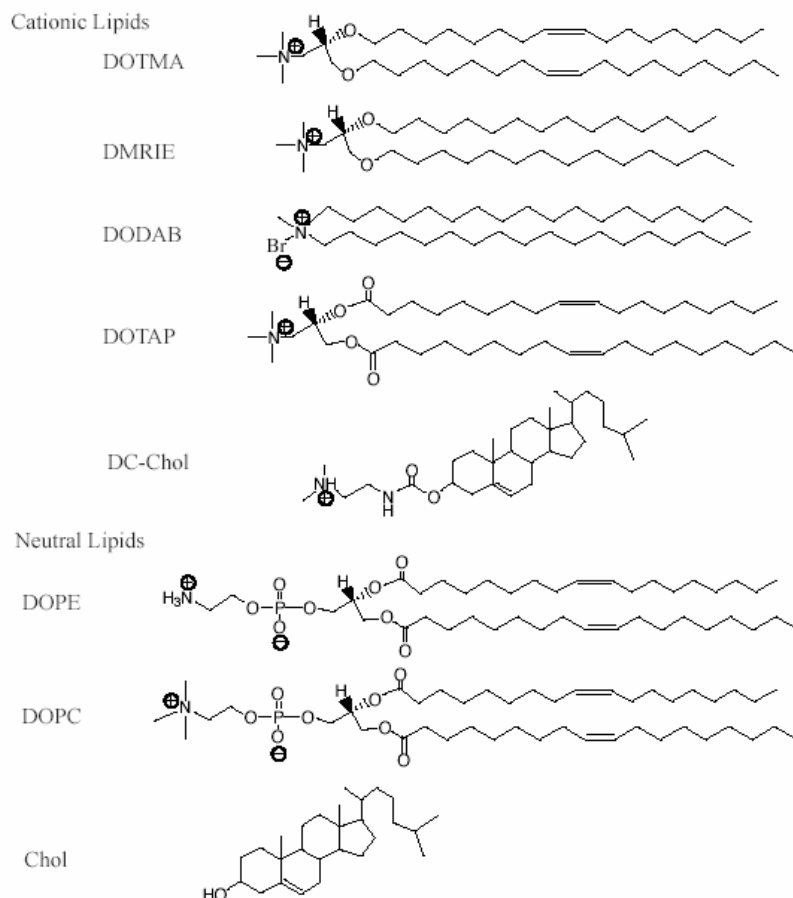
Figure 2: **Structure of common lipids used as materials for gene therapy**. ***Cationic lipids:*** DOTMA:[2,3-bis(oleoyl)propyl]-trimethyl]ammoniumchloride; DMRIE:1,2dimyristyloxypropyl-3-dimethyl-hydroxyethyl ammonium bromide; DODAB: dioctadecyldimethyl ammonium bromide; DOTAP: 1,2-diacyl-3-trimethylammonium propane; DC-Chol: 3[N-(N0,N0-dimethylaminoethane)-carbamoyl] cholesterol. ***Neutral Lipids:*** DOPE: dioleoylphosphatidyl ethanolamine; DOPC: dioleoylphosphatidyl choline; Chol: cholesterol.

Multivalent anions present in the serum or media can facilitate fusion of the lipids causing an increase in the size of the particle. Serum can be a complicating factor for positively charged complexes, possibly causing premature release of the DNA from the complex and enhancing degradation by nucleases. For oligonucleotide + lipid complexes, the various components of serum (e.g., BSA, lipoproteins, macroglobulin) interact with the complexes and alter the complex diameter, zeta potential, and interfere with cellular uptake and nuclear trafficking (**37**). Therefore complexation is generally performed in a serum free medium.

Aggregation of lipoplexes occurs rapidly, which may result in loss of activity in less than 24 hours. Thus, strategies are being developed to stabilize the particles and prolong their shelf life. To improve lipoplex stability, poly-ethylene-glycol (PEG) has been incorporated into the cationic liposome. PEG containing liposomes are prevented from aggregating and interacting with serum components, which increases their stability (**38, 39, 40**).

1.3.2.2 Cationic Polymers:

Cationic polymers have been used since the late 1980's (**41**) as materials for gene delivery. Cationic polymers contain high densities of primary, secondary, tertiary or quaternary amines, some of which are protonatable at neutral pH. This high density of positive charges allows the cationic polymers to form stable complexes with DNA. The cationic polymers assemble with DNA in order to generate condensed structures (40 – 1000 nm in diameter) capable of entering the cell. In addition to providing positive charges for DNA complexation, the primary amines also serve as functional groups to chemically modify the polymers with ligands and peptides that can enhance one or more of the steps in the transfection process.

Poly-L-Lysine:

Poly-L-lysine (PLL) is one of the most commonly used cationic poly amino acids for gene delivery. PLL is typically used at charge ratios (+/-) ranging from 3:1 to 6:1. As increasing amounts of PLL are added to DNA, the structure changes from circular to thick, flattened to compact, and finally to toroid and rod like at a charge ratio of 6:1 (**42**). The diameter and cross section of the toroids are approximately 140 nm and 44 nm respectively. The ideal length of the PLL represents a balance between effective

condensation and Cyto-toxicity. Compared to the low molecular weight PLL, the high molecular weight PLL forms tighter, smaller condensates that are more resistant to the effects of salt concentration and sonication (**43**). However, Cyto-toxicity is inversely related to particle size (**44**). Variation for this exists in case of linear PLL / DNA complexes. Additional information can be found somewhere else (**45**).

Poly(lysine)
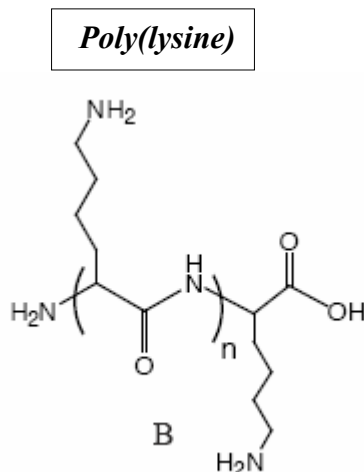
Recent work with poly-amino acids (PAA) focuses on modifications to make them more suitable for gene therapy. For example, the addition of PEG to PLL has shown that PEGylated PLL forms mono-disperse complexes of approximately 25-125 nm in diameter (**46**). PLL was also used in combination with liposomes. DNA is initially complexed with PLL at low charge ratios and cationic lipids are subsequently added to completely condense the DNA. Alternatively, the PLL condensed DNA containing a net positive charge can subsequently be complexed with an anionic lipid (**47**). Pre condensation with PLL has been shown to reduce serum inhibition and also enhance the transfection efficiency (**48, 49**).

Poly Ethylene Imine:

Poly Ehylene Imine (PEI) is perhaps the most widely used cationic polymer to mediate gene delivery due to its high cationic charge density resulting from the protonatable amine on every second carbon (**50**). Its high efficiency of transfection has resulted in two commercially available transfection products ExGene™ and jetPEI®. PEI is synthesized using the acid catalyzed ring opening polymerization of aziridine as either a linear or a branched structure (**51**). Similar to the PLL complexes, low molecular

weight PEI is less Cyto-toxic than high molecular weight PEI. Furthermore, PEI-DNA complexes must also bear a net positive charge (4-13:1 +/- ratio) in order to efficiently transfect cells (**50, 52, 53**). PEI-DNA complexes form spheres or toroids with mean diameters ranging from 30 to 100 nm. The presence of NaCl during complexation can result in particles with amorphous shapes and diameters greater than 1µm.

PEG is used in order to prevent non-specific DNA-cationic polymer complex interactions with serum proteins, cells and tissues in the body, to increase the solubility of the complexes in aqueous milieu, and to prevent the interaction between the DNA-cationic polymer complexes and limit their aggregation in solution (**54**). Traditional cationic polymers for gene delivery such as PEI and PLL have been made more biocompatible using this approach (**54, 55, 56**). Although PEI is one of the most efficient synthetic cationic polymers for gene delivery to date, it is not biodegradable and can have significant Cyto-toxicity both *in vitro* and *in vivo*. In an effort to increase the biocompatibility of PEI, low molecular weight PEI was cross-linked with degradable PEG polymer (**55**). Low molecular weight PEI was cross-linked with di-functional PEG to form PEI-PEG-PEI. The molecular weights of the starting PEI polymers were 600, 1200, 1800 Da, while the molecular weight of the di-functional PEG derivative was kept constant. Cyto-toxicity experiments showed decreased Cyto-toxicity for complexes formed with degradable PEI/DNA complexes when compared to complexes formed with 25kDa PEI.
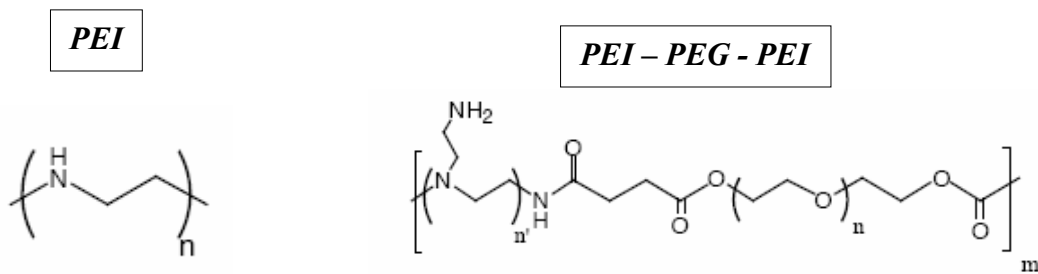
1.4 Peptides in gene delivery:

1.4.1 Arginine (Arg) rich peptides in gene delivery:

Recently, methods have been developed for the delivery of exogenous proteins into living cells with the help of membrane permeable carrier peptides. By genetically or chemically hybridizing these carrier peptides, efficient intracellular delivery of various oligopeptides and proteins was achieved. The use of HIV-1 Tat (48-60) and Drosophila Antennapedia (43-58) in delivering peptides (β-galactosidase) and fluorescence probes to various tissues in mice including the brain, augments their use as tools not only in therapeutic purposes but as an alternative to gene delivery (**57, 58**). Besides HIV-1 Tat, Antennapedia and Herpes simplex virus type-1 VP22 transcription factor, various RNA binding, DNA binding proteins and simply poly-Arginines (R_4 to R_{16}) are used in various studies.

RNA-binding peptides:	
HIV-1 Rev (34-50)	TRQARRNRRRRWRERQR
FHV(floch house virus) coat (35-49)	RRRRNRTRRNRRRVR
BMV(brome mosaic virus) Gag (7-25)	KMTRAQRRAAARRNRWTAR
HTLV-II(human tcell lymphotropic)Rex(4-16)	TRRQRTRRARRNR
	MDAQTRRRERRAEKQAQWKAAN
λN(1-22)	TAKTRYKARRAELIAERR
Ø21 N (12-29)	TRRNKANRIQEQLNRK
Yeast PRP6 (129-144)	
DNA-binding peptides:	
Human c-Fos (139-164)	KRRIRRERNKMAAKSRNRRRELTDT
Human c-Jun (252-279)	RIKAERKRMRNRIAASKSRKRKLERIAR
Yeast GCN4 (231-252)	KRARNTEAARRSRARKLQRMKQ

Table 1: **Arginine rich peptides:** Number of Arg decreases down the table in each type and so does their internalization efficiencies

Arg rich basic segments are used by a variety of RNA binding proteins to recognize specific RNA structures. Futaki. S et al., showed that peptide translocation through the cell membrane and accumulation in cytoplasm and nucleus showed a tendency to correspond to the number of Arg residues in the sequence. Similar effects were also observed with the DNA-binding peptides corresponding to the basic Leucine

zipper segments derived from cancer related proteins (c-Fos, c-Jun) and yeast GCN_4, which were also rich in Arg. There seems a common or very similar mechanism for the internalization among these peptides. The mechanism is explained neither by adsorptive mediated nor receptor mediated endocytosis, because the peptides were shown to have internalized by cells at $4^{o}C$, and there seemed little homology both in the primary and secondary structures among these peptides (as shown by their Circular Dichroism spectra) except that they have several Arg residues in their sequence. Studies on application of poly-Arginines (R_4 to R_{16}) suggest that an optimal number of Arg residues (6-10) are required for efficient internalization. There still remains a question why such efficient translocation is possible for Arg rich peptides? Possible hydrogen bond formation with lipid phosphates or interaction with extra-cellular matrices such as heparin sulphate may be involved in the initial steps during the mechanism. However, failure of internalization of peptides $>R_{10}$ residues suggest that it is not enough to explain the mechanism only by considering adsorption of peptides on the membranes (**59**).

1.4.2 Tat (Transcriptional activator protein):

The HIV-1 (Human immunodeficiency virus type1) is a retrovirus belonging to the *Lentiviridae* family. The genome of most retrovirus encodes the conserved structural and enzymatic genes encoding the Gag, Pol and Env proteins. In addition to these, HIV-1 contains two additional regulatory genes (tat and rev) and four accessory genes (vif, vpu, vpr, and nef). These additional genes differentiate lentivirus from oncovirus.
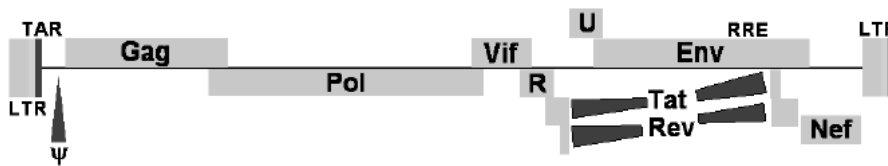
Figure 3: **Wild type HIV-1 genome organization.**

Tat is a transcriptional activator that binds to a short nascent stem-bulge-loop leader RNA, TAR (trans-activation responsive), for its activity. The 101-amino acid Tat protein, with residues 1–72 encoded by a first exon and residues 73–101 encoded by a second exon, can be arbitrarily considered as containing several "domains" of interest. It should be noted that an 86 amino acid form of Tat exists in a few laboratory passaged

virus strains (e.g. LAI, HXB2, pNL4–3). These versions represent a truncated and non-natural full-length protein. Although residues 87–101 of Tat might not contribute greatly to the *ex vivo* propagation of HIV-1, their conservation in viruses that replicate *in vivo* provides a good indication of their biological importance. (**60**)

Figure 4: **Physical domains of the 101-amino acid HIV-1 Tat protein.** Tat can be broadly viewed as containing five physical domains. The underlying illustration highlights that the popularly considered full-length Tat protein (86 amino acids) based on the open reading frames from laboratory passaged viruses (LAI, HXB2, and NL4–3) is likely missing for the carboxyl-terminal 87–101 amino acid residues, which are conserved in natural isolates of HIV-1 that replicate *in vivo*. Thus it has been shown that a single nucleotide change in the stop codon of *Tat* from laboratory isolates, LAI, HXB2, and NL4–3, converts these open reading frames to the 101-amino acid sequence (*e.g.* SF2) found in Tat from natural viral isolates.

The best-studied region of Tat resides in amino acids 49–72 (domain 4), which contain a basic RKKRRQRRR motif. This peptide motif confers TAR RNA binding properties to Tat (32–35), which is important for the nuclear localization and uptake of Tat by the cells. For association with TAR, the short basic motif contributes importantly to affinity but dictates insufficiently to the specificity of binding. Flanking amino acids outside this basic domain significantly influences the specificity of Tat-TAR interaction. (**60**)

1.4.2.1 Role of Tat in HIV-1 LTR- directed transcription:

Transcription from the HIV-1 LTR is several hundred folds higher in the presence of Tat than in its absence. Optimal Tat action requires in addition to TAR RNA, basal (TATA) and upstream promoter elements (e.g. Sp1). In considering Tat action, one should understand that two operationally defined events occur for each round of transcription at virtually all promoters. These are: (i) recruitment of an RNA polymerase II (RNAP II) complex to the promoter and (ii) the escape of that complex from the promoter into productive elongation. Several models of Tat transactivation have been proposed. The following are the two widely accepted ones. (**60**)
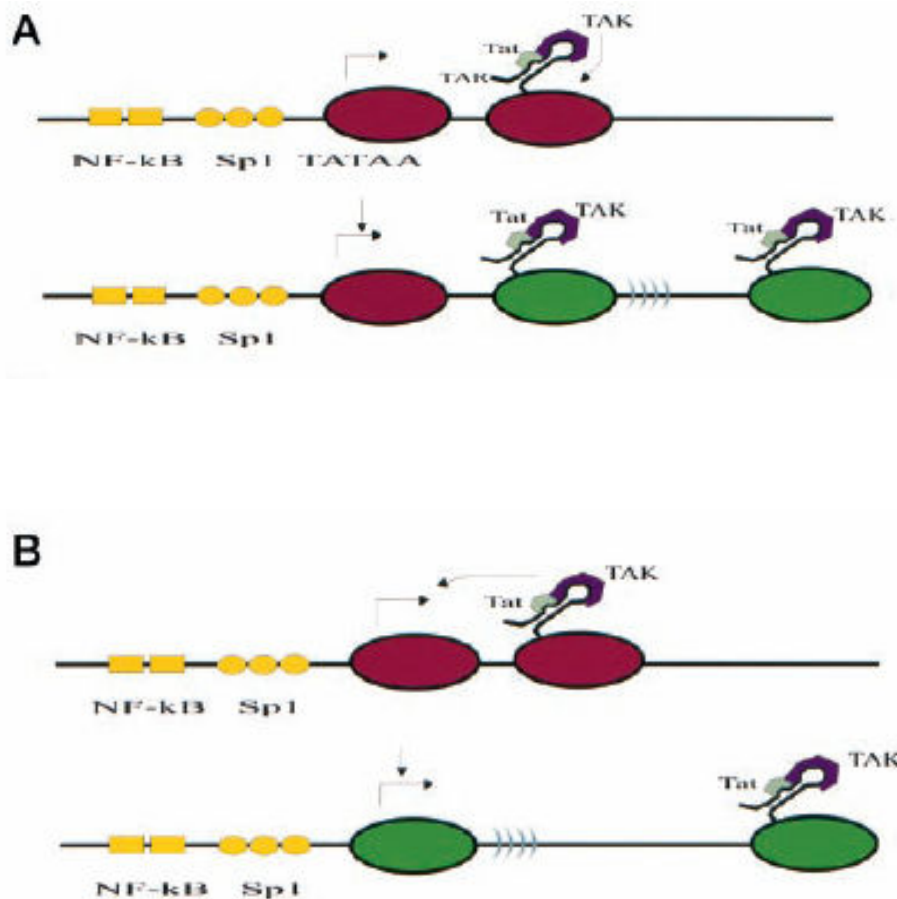
Figure 5: **Schematic models of Tat transactivation:** A simplified representation of the HIV-1 promoter containing two (*small yellow rectangles*) NF-kB-binding sites and three (*small yellow ovals*) Sp1-binding sites. *Large ovals* represent RNAP II complexes that overlie the TATAA box and transcribe a promoter-proximal stem-bulge-loop TAR RNA. Tat (*gray*) binds the bulge of TAR, whereas TAK (*purple*) binds the loop of TAR. In *A*, loop-bound TAK is shown to phosphorylate RNAP II in its CTD domain converting a non-processive (*red*) to a processively elongating (*green*) polymerase. Here, it is suggested that TAK acts on a paused RNAP II

molecule which has cleared the promoter. ***B*** diagrams an alternate view whereby protein(s) bound to the TAR loop of an early elongating RNAP II affects the activity of a subsequent RNAP II that is yet docked at the promoter, converting a non-productive (*red*) to a productive (*green*) complex. In this perspective, an activity of TAR-bound proteins serves to facilitate promoter clearance. The activities in *A* and *B* need not be mutually exclusive.

1.4.2.2 Role of Tat in cellular uptake:

Several studies have shown that exogenous Tat protein was able to translocate through the plasma membrane and to reach the nucleus to trans-activate the viral genome. A region of the Tat protein centered on a cluster of basic amino acids has been assigned to this translocation activity. Recent data have demonstrated that chemical coupling of a Tat derived peptide (37-72 of domain 4) to several proteins allowed their functional internalization into several cell-lines or tissues. A part of this domain can be folded in a α-helix structure with amphipathic characteristics. Such helical structures have been considered as key determinants for the uptake of several enveloped viruses by fusion or endocytosis (**61, 62, 57**). Rudolph. C et al., have shown that oligomers of Tat peptide, compacts plasmid DNA to nanometric particles and stabilizes the DNA from nuclease degradation (**63**). Recent data have shown that, HIV-1 virus itself or full-length Tat may exploit a caveoli-mediated pathway for cellular internalization and is inhibited at 4°C. The exact pathway(s) of Tat peptide resulting in nuclear localization is however unexplained. (**64, 65**)

1.4.3 Integrin-targeting:

RGD has high affinity towards integrin receptors - αVβ3, α5β1 expressed on cell surfaces and therefore may improve DNA binding to cells. Albinsson. B et al., studies on Adenovirus type 41 lacking an RGD alpha (v)-integrin binding motif on the penton base, showed a delayed uptake in A549 cells. Various studies in different cells have shown an enhancement of integrin-mediated transfection with synthetic vector systems containing RGD motifs (**66**)

S.No	Integrin target	Sequence
1	α3I, α5β1, αVβ3, αVβ5, αIIBβ3	GAC**RGD**MFGCA
2	α5β1	GACRRETAWACG

Table 2: **Peptide sequences and receptor targets.**

Integrins are a family of more than 20 heterodimeric membrane proteins that bind to extracellular matrix proteins. Integrins play an important role in cellular activities such as cell-cell interactions, attachment of the cells to the basement membrane and cell motility. A diverse range of pathogens, including bacteria and viruses, exploits Integrin receptors, for their cell binding and entry. On this basis it was proposed that integrin-targeting might also be an efficient pathway for the uptake of synthetic gene delivery vehicles. Cellular distribution patterns of the 20 or so known heterodimers vary, with some, being wide spread in their cellular distribution such as α3β1 and others being more restricted, such as αMβ2 which occurs on macrophages only. Integrin expression and activation patterns may be altered in disease processes such as lung inflammation, cancers, allowing further specific targeting opportunities. Exogenous agents such as cytokines and phorbol esters may activate some integrins, including the fibronectin receptors α4β1 and α5β1. Activated integrins have higher ligand-binding affinity, which therefore may enhance the efficiency of vectors targeted to these integrins (**67**).

1.5 Application: *RELM-β as hypoxia induced mitogenic factor.*

Pulmonary vascular remodeling, characterized by pulmonary micro-vascular smooth muscle cell proliferation, is implicated in the development of hypoxic pulmonary artery hypertension (PAH). Broncho-alveolar lavage (BAL) fluid from mice with experimentally induced allergic pulmonary inflammation revealed a novel 9.4 kDa cysteine rich secreted protein, FIZZ1 (found in inflammatory zone) (**68**).

FIZZ1 is a recently described protein in rodents, and belongs to a novel class of cysteine rich proteins known as the FIZZ family. The murine FIZZ genes are expressed in distinct tissue specific patterns, implying divergent biological activities. Murine FIZZ2 (mFIZZ2) is found exclusively in the actively replicating crypt epithelium of the small and large intestine. Murine FIZZ3 (mFIZZ3) is expressed uniquely in white adipose tissue through out the body. Murine FIZZ1 (mFIZZ1) is expressed in at least two tissues: the lung epithelium and non-neuronal cells adjacent to neurons, particularly in the submucosa of the gut and peribronchial stroma. In lung mFIZZ1 expression is specific to bronchial mucosal epithelial cells and type II alveolar pneumocytes. Increased expression in bronchial epithelial and type II pneumocyte, in allergen-induced inflammation suggests the role of mFIZZ1 in respiratory epithelial cell maintenance and response to injury (**68**). Although human FIZZ2 and FIZZ3 have been reported, there is yet no known human homologue of FIZZ1 (**69**).

FIZZ3 was shown to be implicated in type II diabetes mellitus and was renamed as resistin (**70**). FIZZ1 and FIZZ2 were renamed as resistin-like molecule α (RELMα) and β (RELMβ) respectively. Resistin shows no significant sequence identity to previously characterized proteins and exhibits similarity only to the other family members, RELMα, RELMβ and the recently discovered RELMγ. Phylogenomics revealed that the human resistin gene is the ortholog of its murine counterpart and is located in a region of chromosome 19p13.3, which is syntenic to mouse chromosome 8A1. In addition to the RELM sequences already reported, bioinformatic analysis disclosed another RELM sequence in the vicinity of RELMβ on human chromosome 3q13.1, but this sequence is unlikely to encode an expressed gene. Therefore, only two RELMs- resistin and RELMβ, exist in humans, instead of the three RELMs- resistin, RELMα, and RELMβ that exist in

mice. This study suggests that the RELM family is not well conserved in evolution and may function differently between species (**71**).

Xingwu Teng et al., hypothesized that mFIZZ1 participates in the process of hypoxia-induced pulmonary remodeling. mFIZZ1 could be induced at or near the pulmonary vasculature by hypoxia, and the secreted mFIZZ1 might have a proliferative effect on the pulmonary vascular smooth muscle cells. mFIZZ1 was found to be markedly induced by hypoxia in the pulmonary vasculature as well as in bronchial epithelial cells and type II pneumocytes. mFIZZ1 was shown to stimulate pulmonary smooth muscle cell proliferation, and so it was renamed as hypoxia induced mitogenic factor (HIMF) (**72**). Recent studies have shown that HIMF expression is induced in compensatory lung growth and that intra-tracheal instillation of HIMF protein induced wide spread cell proliferation in mouse lung (**73**).

Aim of the work:

Efficient DNA transfection is critical for biological research and new clinical therapies. Current non-viral transfection methods, empirically designed to maximize DNA complexation and/or membrane fusion, are amenable to enhancement by a variety of chemicals. Most chemical enhancements produce a moderate increase in gene delivery and a limited increase in gene expression, which is a primary requisite for various studies. Further more, the toxicity associated with these agents also circumscribe their utility especially on primary cells. In the present study we employed a synthetic conjugate peptide TatRGD (TR) as a vehicle for gene delivery in pulmonary cell-lines and primary cells. We applied these vectors to study the role of RELMβ as hypoxia induced mitogenic factor

Specific Aim 1: Generation of non-viral gene transfer mode for pulmonary cell-line and primary cells, with vector systems containing synthetic conjugate peptide, TatRGD and observing the role of caveoli in the cellular internalization of these vectors. To meet this aim the following approaches were undertaken:

1. Synthesis of conjugate peptide TatRGD following *F-moc* strategy and HPLC purification.

2. Analysis of TR and DNA binding.

3. Particle size measurements for TRD (TatRGD/ DNA) and TRDL (TatRGD/ DNA/ cationic Lipid) using zeta sizer.

4. Cyto-toxicity assays for TRD and TRDL vectors.

5. Dosage optimisation for TRD and TRDL vectors.

6. Analysis of DNA uptake using gene scan.

7. Comparison of transfection efficiencies of TRDL vectors with that of other commercial transfection agents employed.

8. Analysis of the role of Caveoli in the cellular internalization of TRDL vectors employing immuno-staining and laser scanning confocal fluorescence imaging techniques.

Specific Aim 2: Application of TR mediated gene transfer in studying the role of RELMβ as a candidate gene responsible for pulmonary vascular cell proliferation or in hypoxia related fibrotic lung diseases. To meet this aim the following approaches were undertaken.

1. Isolation and cloning human RELMβ cDNA from human lung tissue.

2. Expression analysis of RELMβ in various human tissues.

3. Regulation of RELMβ in A549, FB_{PA} and SMC_{PA} cells by semi-quantitative and quantitative RT-PCR.

4. Over-expression of RELMβ employing TRDL and DL vectors and subsequent analysis by western blotting and proliferation assays.

2.1 Materials:

2.1.1 Cell biology materials:

2.1.1.1 Cells:

A549 (Human Caucasian lung carcinoma cells): A549 cells are derived from a 58 year old Caucasian male. These cells can synthesise lecithin utilising the cytidine diphosphocholine pathway. Occasionally, cells may also contain inclusion bodies although they are not known to carry any human pathogen.

Morphology: Epithelial. Depositor: Obtained from ATCC, USA.

Fb_{PA} (Human pulmonary artery fibroblast cells) and SMC_{PA} (Human pulmonary artery smooth muscle cells): Primary cells were isolated from the human pulmonary artery. Human primary cell preparations were established from lung tissue obtained from patients undergoing lung transplantation with their due consent. This protocol was approved by the Justus-Liebig-University ethics committee. Cells of passage 2 and 3 were used.

2.1.1.2 Cell culture:

OptiMEM + glutaMAX (GIBCO)

Trypsin 1x: It is a proteolytic enzyme. Trypsin usually in combination with EDTA; causes cells to detach from the growth surface. The proteolysis reaction can be quickly terminated by the addition of complete medium containing serum.

Component	Volume
Trypsin 10x	10 ml
200mM HEPES	10 ml
0.9% NaCl	80 ml
Total	**100 ml**

Culture Medium:

Medium Components	A549	Fb_{PA} and SMC_{PA}
Medium	DMEM(F12)Nutrient Mix	MCDB 131
Antibiotic (Pen-Strep)	1%	1%
Glutamine	1%	1%
Non-Essential A.a	1%	
EGF		0.5ng/ml

BFGF		2ng/ml
Insulin		5μg/ml
Vitamins	1%	
FCS	10%	5%

Table 3: Medium composition for A549, FB$_{PA}$ and SMC$_{PA}$ cells.

2.1.1.3 Transfection agents:

Magnetofections reagent (Chemicell): CombiMAG/L-200 is a ready to use magnetofection reagents. It can be combined with any poly-cationic and lipidic transfection reagent, and also with adenoviral and retroviral vectors.

MagnetoFACTOR plate (Chemicell): Apart from suitable magnetic nano-particles, magnetofection requires appropriate magnetic fields. These are provided by the MagnetoFACTOR plate, especially designed for magnetofection.

Polyethylenimine (PEI), high molecular weight, water-free (ALDRICH): PEI is a branched polymer. Average molecular weight: 25,000. Density: 1.03g/ml at 25°C.

Formula:

$$\left(-NH\ CH_2\ CH_2\ \right)_x \left(-N-CH_2\ CH_2\ - \atop | \atop CH_2CH_2NH_2 \right)_y$$
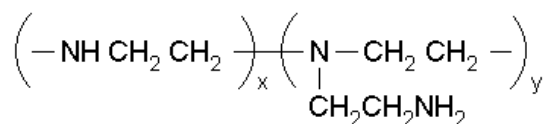
Lipofectamine™ 2000, 1mg/ml (Invitrogen): Lipofectamine™ 2000 is a cationic lipid suitable for the transfection of nucleic acids into eukaryotic cells. Use of Lipofectamine™ 2000 provides high transfection efficiency in many cell types and formats (e.g. 96-well). It can be added directly to cells in culture medium (in presence or absence of serum). Complexes can be removed after 4-6 hours without loss of activity.

TatRGD Conjugate peptide diluted to 2mg/ml.

2.1.2 Molecular biology materials:

2.1.2.1 Bacterial strains:

TOP10 bacterial strain from Invitrogen was used for plasmid transformation. Genotype of the strain is "*F-mcrA. (mrr-hsdRMS-mcrBC) Φ80lacZ. M15. lacX74 recA1 araD139. (araleu) 7697 galU galK rpsL (StrR) endA1 nupG* "

2.1.2.2 Vectors:

pGL3-CMV vector: The pGL3-basic vector was used for obtaining pGL3-CMV vector. The CMV fragment was cloned using *Sal I* and *BamH I* restriction sites in pGL3-basic vector. Expression of luciferase activity in cells transfected with this plasmid is due to proper orientation of CMV promoter upstream from luc+. This vector also contains ColE1 ori, f1 ori, ampicillin resistance gene and MCS.

pEGFP Vector: pEGFP-N1 vector was used for transfecting cells and checking their transfection efficiency through the emission of green fluorescence. Plasmid pEGFP-N1 encodes a red-shifted variant of wild-type GFP (1–3) which has been optimized for brighter fluorescence and higher expression in mammalian cells. (Excitation maximum = 488 nm, emission maximum = 507 nm). The MCS in pEGFP-N1 is between the immediate early promoter of CMV (PCMV IE) and the EGFP coding sequences.

pGEM®-T Easy vector: The vector pGEM®-T Easy (Promega, Madison USA) was used for the cloning and sequencing of PCR products. The vectors are prepared by cutting Promega's pGEM®-T Easy Vectors with EcoR V and adding a 3´ terminal thymidine to both ends. These single 3´-T overhangs at the insertion site greatly improve the efficiency of ligation of a PCR product into the plasmids by preventing recircularization of the vector and providing a compatible overhang for PCR products generated by certain thermo stable polymerase. These polymerases often add a single deoxyadenosine, in a template-independent fashion, to the 3´-ends of the amplified fragments. It contains ColE1 ori for the replication in *E coli*, the Ampicillin resistance gene for antibiotic selection, f1 ori for single strand DNA production, the LacZ gene encoding β-galactosidase which provides the possibility for blue/white color selection of

recombinant clones, a multiple cloning site (MCS), T7 and SP6 RNA polymerase promoters for DNA sequencing.

pCMV-HA vector: The pCMV-HA vector was used in the experiments for tagging the protein of interest with an HA epitope. This vector also contains ColE1 ori, f1 ori, ampicillin resistance gene and HA epitope sequence followed by MCS.

2.1.2.3 Oligonucleotides:

The oligonucleotides were obtained from Metabion (Martinsried, Germany) at the synthesis scale: 0.02 μmol.

Oligonucleotides for PCR and Cloning:

Fam-CMV (400bp)
Fam CMV- : 5′ *Fam*- ATG GAA AGT CCC TAT TGG CGT 3′
Pgl3 + : 5′ CTG TCC CCA GTG CAA GTG CA 3′

CMV (400bp)
CMV- : 5′ ATG GAA AGT CCC TAT TGG CGT 3′
Pgl3+ : 5′ CTG TCC CCA GTG CAA GTG CA 3′

RELMβ
Full length RELMβ (F) (for cloning in pGEM-T easy)
M-HIMF-f: 5′ AAA CTG AGT TCT CAG CCT CCT C 3′
P-HIMF-f: 5′ CCC CAG GAC ACT GAC TCT GTA 3′

RELMβ (for cloning in pCMV-HA)
HIMF-kozak-kpn1: 5' ctt ggt acc gcc gcc acc ATG GGG CCG TCC TCT TGC CTC C 3'
HIMF-HA-TGA-xho1: 5' gaa ctc gag tca gcc gcc acc agc gta atc tgg aac atc gta tgg gta gcc ACC GGT CAG GTG GCA GCA GCG GGC AGT GGT CC 3'

Oligonucleotides for RT-PCR and Real time RT-PCR:

HIMF
hs HIMF – 362 - : 5′ CCA CGA ACC ACA GCC ATA G 3′
hs HIMF – 145+ : 5′ CCC TTC TCC AGC TGA TCA AC 3′

HPRT
HPRT –: 5′ TCA AAT CCA ACA AAG TCT GGC CTG T 3′
HPRT +: 5′ TCG AGA TGT GAT GAA GGA GAT GGG A 3′

Oligonucleotides for Sequencing:

pGEM®-T Easy

T7: 5´ TAATACGACTCACTATAG 3`

SP6: 5´ATTTAGGTGACACTATAGAA 3`

pCMV – HA
Forward: 5´ AGT GTT ACT TCT GCT CTA AAA GCT GC 3´
Reverse: 5´ CAC TGC ATT CTA GTT GTG GTT TGT 3´

2.1.2.4 Enzymes:

Restriction endonucleases:

All restriction endonucleases were obtained from Roche Diagnostics GmbH, Mannheim, Germany. Their activity was optimized in their respective buffers provided by the company. The characters of restriction endonucleases were described as follows:

Enzyme Specificity Buffer

Enzyme	Sequence	Buffer
Xho I	5' C↓TCGAG 3'	10mM Tris HCl (pH 8), 5mM MgCl$_2$, 100mM NaCl, 0.1mg/ml BSA
Kpn I	5' GGTAC↓C 3'	10mM Tris HCl (pH 7.5), 10mM MgCl$_2$, 0.1mg/ml BSA

HotstarTaq DNA-Polymerase

HotstarTaq DNA Polymerase (Qiagen Inc, Hilden, Germany) is a modified form of *Taq* DNA polymerase that is supplied in an inactive state that has no polymerase activity at ambient temperatures. This prevents extension of nonspecifically annealed primers and primer dimers formed at low temperatures during PCR setup and the initial PCR cycle. *HotstarTaq* DNA Polymerase is activated by 15 min incubation at 95°C that can be incorporated into thermal-cycler program. Hotstar *Taq* DNA polymerase is a 5'-3' DNA polymerase and has no 3'-5' and 5'-3' exonuclease activity.

CIP (Calf Intestinal Alkaline Phosphatase)

Alkaline Phosphatase catalyzes the removal of 5´ phosphate groups from DNA, RNA, ribo and deoxyribonucleoside triphosphates. Since CIP treated fragments lack the

5´phosphoryl termini required by ligases, they cannot self-ligate. This property can be used to decrease the vector background in cloning experiments.

T4 DNA ligase

T4 DNA ligase was purchased from Roche Diagnostics GmbH, Mannheim, Germany. This enzyme catalyzes the formation of a phosphodiester bond between the 5' phosphate of one strand of DNA and the 3' hydroxyl group of the other. This enzyme is used to covalently link or ligate fragments of DNA together. Most commonly, the reaction involves ligating a fragment of DNA into a plasmid vector.

RNase A

Bovine pancreatic ribonuclease A (RNase A) was also purchased from Roche Diagnostics GmbH, Mannheim, Germany. It is a small monomeric enzyme of 124 amino acids and a molecular weight of 13.7 kDa. The function of this enzyme is to hydrolyze single-stranded RNA by cleaving the phosphodiester bond. It results in formation of nucleoside 5'-monophosphates. RNase A has a pH optimum at 7.0 - 7.5 (Sambrook & Russell 2001). It is used in the isolation of DNA. To inactivate DNases, the RNase A solution should be heated before use for 10 min at 100° C.

DNase I

DNase I is a versatile enzyme that nonspecifically cleaves DNA to release 5'-phosphorylated di-, tri-, and oligonucleotide products. It is a powerful research tool for DNA manipulations used in a range of molecular biology applications. Some of its uses include: Degradation of contaminating DNA after RNA isolation, "Clean-up" of RNA prior to RT-PCR and after in vitro transcription, Identification of protein binding sequences on DNA (DNase I footprinting), Prevention of clumping when handling cultured cells, and Creation of a fragmented library of DNA sequences for in vitro recombination reactions.

2.1.2.5 Antibodies and Fluorescent dyes:

Antibodies and fluorescent dyes used in the experiments are all commercially available. Their parameters were described

For Western-blot analysis

Primary antibodies:

Anti-HA (monoclonal) mouse (Sigma, Seelze, Germany)

Anti-human β-Actin (monoclonal) mouse (Abcam, Cambridge, UK)

Secondary antibody:

Anti-mouse IgG sheep, biotin conjugated (Bio-Rad, München, Germany)

For immuno-staining:

Primary antibody

Caveolin-1(N-20)sc-894: Anti-Cav-1(polyclonal) rabbit (Santa Cruz Biotechnology).

Secondary antibodies

Anti-rabbit IgG donkey, Cy5 conjugated, # 62771 (Dianova)

Anti-rabbit IgG donkey, Cy-3 conjugated, # 63631 (Dianova)

Streptavidin Cy-3 conjugated, # 59606(Dianova)

WGA-633: It is a membrane staining dye. Wheat germ agglutinin W-21404, conjugated with Alexa Flur 633 (Molecular Probes, OR, USA). λ-Abs: 632nm and λ-Em: 647nm.

TO-PRO3: It is a nuclear staining dye (Molecular Probes). λ-Abs: 642nm and λ-Em: 661nm.

2.1.3 Detection and purification systems (Kits):

Kit	Provider
Nucleobond, Plasmid purification system	MACHEREY-NAGEL / Düren, Germany
QIAEXII gel extraction kit	Qiagen / Hilden, Germany
QIAquick PCR purification kit	Qiagen / Hilden, Germany
BigDye® terminator v3.1 sequencing	Applied Biosystems / Darmstadt, Germany
ECL-kit	Amersham / Freiburg, Germany
AB complex/HRP	DakoCytomation / Hamburg, Germany
Luciferase reporter assay kit	Promega / Mannheim, Germany
MTT cell proliferation assay	Promega / Mannheim, Germany
CytoTox-ONE membrane integrity assay	Promega / Mannheim, Germany

Table 4: Detection and purification systems (Kits)

2.4 Methods:

2.2.1 Cell biology methods:

2.2.1.1 Culturing human A549, FB$_{PA}$ and SMC$_{PA}$ cells:

The culturing of the human pulmonary epithelial cell line A549 was performed according to the protocol given by the American Type Culture Collection. Human Pulmonary artery adventitial fibroblasts (FB$_{PA}$) and Smooth muscle (SMC$_{PA}$) cells were isolated and cultured as described (**74**). The cells frozen in DMSO at -70°C (app. 5×10^6 cells) were thawed at 37°C and then transferred into a 100 mm dish containing app. 12 ml of A549 medium. When the cells became confluent, they were treated with 1x trypsin. The reaction was stopped by adding 10 ml of medium with 10% FCS (contains trypsin inhibitors). For further culturing about $1/3^{rd}$ of the volume of medium containing cells were transferred to a fresh plate and cultured in gas controlled incubators in water vapor saturated atmosphere with 1% O_2 (v/v) or atmospheric O_2 (v/v), 5% CO_2 and, accordingly, 94% (v/v) or atmospheric N_2 at 37°C in normbaric conditions. The cells were usually confluent in 3 days. Cells were plated in different sized plates based upon its down stream application, as follows:

Slide / Plate size	**No.of cells**	**Application**
100 mm plate	5×10^6	DNA / RNA isolation
6 well plate	5×10^5	*Fam*-DNA / Protein isolation
24 well plate	1.5×10^5	Transfections/ Reporter assay
96 well plate	2.5×10^4	Magnetofection/ transfection/Cyto-toxicity
8 well culture slide	0.5×10^5	Immunostaining

2.2.1.2 Transfections:

Magnetofection:

Approximately 2.5×10^4 Cells/ well were added in a 96-well plate and cultured overnight at 37°C in CO_2 incubator. The cells were 85-90% confluent for transfection on the following day. 0.2 µg/well DNA was diluted in 25µl Opti-MEM® serum free medium. 0.5µl/well lipofectamine.2000 was diluted in 25µl Opti-MEM® medium. Mixtures were incubated for 5 m at room temperature. The diluted DNA was slowly added to the diluted

lipofectamin 2000, mixed and incubated for 15 m at room temperature to facilitate the formation of DNA-Lipofectamine (DL) complexes. The CombiMAG/L-200 magnetofection reagent was vortexed before use. 0.8µl/well CombiMAG/L-200 reagent was added to the DL mixture and incubated at room temperature for 15 m. The DL-Mag complexes were added to the cells and the 96-well plate was placed over the 96-well magnetofactor plate for 15 m for cell-lines and 5-10 m for primary cells. Following the incubation over the magnetofactor plate the DL-Mag mixture was replaced by culture medium and the cells were incubated at 37°C in CO_2 incubator overnight.

PEI mediated transfection:

Stock solution of PEI was prepared by dissolving PEI in water. The resultant stock solution (2mg/ml) was then filter sterilized. The following formula was employed to calculate the amount of PEI, from the stock solution to be used per µg DNA. The calculations are based on the N/P ratio to be employed. N/P ratio was standardized to 4 after trying N/P ratios ranging from 3 to 6. Higher N/P ratios suggest higher cationic behavior and also higher toxicity.

PEI Formula:

[(x µg DNA × 43.1µg per µmol) ÷ 330µg per µmol] × [(y) N: P ratio ÷ 2 (concentration of stock solution in mg/ml)]

Therefore: [(1 × 43.1) ÷330] × [4 ÷2] = 0.26µl from 2mg/ ml stock solution for 1µg DNA.

The cells were plated in the desired culture plates following the specifications mentioned in the table in section 2.2.1.1 and cultured overnight at 37°C in CO_2 incubator to attain 85-90% confluence for transfection on the following day. DNA was diluted in 150mM NaCl (4µg in 125µl/well for 6-well plate, 1µg in 25µl/well for 24-well plate and 0.2µg in 12.5µl/well for 96-well plate). PEI from the stock solution was diluted in 150mM NaCl (1.04µl in 125µl/well for 6-well plate, 0.26µl in 25µl/well for 24-well plate and 0.05µl in 12.5µl/well for 96-well plate). Mixtures were incubated for 10 m at room temperature. The diluted PEI was slowly added to the diluted DNA, mixed and incubated for 10 m at room temperature to facilitate the formation of PEI-DNA complexes. Corresponding amounts (250µl/well for 6-well plate, 100µl/well for 24-well plate and 50µl/well for 96-well plate) of the PEI-DNA complexes were added to the cells and an equal volume of

OptiMEM was also added to prevent drying of the cells. The cells were incubated at 37°C in CO_2 incubator for 4 h. After 4 h the medium was replaces with culture medium and the cells were incubated at 37°C in CO_2 incubator overnight.

Lipofectamine 2000 mediated transfection:

The cells were plated in the desired culture plates following the specifications mentioned in the table in section 2.2.1.1 and cultured overnight at 37°C in CO_2 incubator to attain 85-90% confluence for transfection on the following day. DNA was diluted in Opti-MEM® serum free medium (4µg in 250µl/well for 6-well plate, 1µg in 50µl/well for 24-well plate and 0.2µg in 25µl/well for 96-well plate). Lipofectamine.2000 was diluted in Opti-MEM® medium (10µl in 250µl/well for 6-well plate, 2µl in 50µl/well for 24-well plate and 0.5µl in 25µl/well for 96-well plate). Mixtures were incubated for 5 m at room temperature. The diluted DNA was slowly added to the diluted lipofectamin 2000, mixed and incubated for 15 m at room temperature to facilitate the formation of DNA-Lipofectamine (DL) complexes. Corresponding amounts (500µl/well for 6-well plate, 100µl/well for 24-well plate and 50µl/well for 96-well plate) of the DL complexes were added to the cells and incubated at 37°C in CO_2 incubator for 4 h. After 4 h the medium was replaces with culture medium and the cells were incubated at 37°C in CO_2 incubator overnight.

TRD and TRDL mediated transfection:

The cells were plated in the desired culture plates following the specifications mentioned in the table in section 2.2.1.1 and cultured overnight at 37°C in CO_2 incubator to attain 85-90% confluence for transfection on the following day. DNA was mixed with TatRGD (2, 4, 6, 12.5, 25µg for dosage curve) and the volume was made up with HBS (50mM NaCl and 10mM HEPES). The TatRGD-DNA (TRD) mixture was vortexed and incubated at room temperature for 15 m. The resulting mixture was directly used for TRD mediated transfection or used for preparation of TatRGD-DNA-Lipofectamine (TRDL) complex mixture. Specified amount of lipofectamine was added to the TRD mixture and incubated at room temperature for 15 m, in order to form the TRDL complex mixture.

Corresponding amounts of the TRD or TRDL mixtures were added to the cells and incubated at 37°C in CO_2 incubator for 4 h. After 4 h the medium was replaces with culture medium and the cells were incubated at 37°C in CO_2 incubator overnight.

Plate/slide	(TR-D,TR-D-L/ well) **Cell-lines**	(TR-D-L/ well) **Primary cells**
6-well	4µgDNA+48µgTR+HBS(250µl)+**10µlLipo**	4µgDNA+16µgTR+HBS(250µl)+10µlLipo
24-well	1µgDNA+12.5µgTR+HBS(75µl)+**2µlLipo**	1µgDNA+4µgTR+HBS(75µl)+2µlLipo
96-well	0.2µgDNA+2.5µgTR+HBS(25µl)+**0.5µlLipo**	0.2µgDNA+0.8µgTR+HBS(25µl)+0.5µlLipo
8-chamber	0.5µgDNA+6µgTR+HBS(50µl)+**1µlLipo**	0.5µgDNA+2µgTR+HBS(50µl)+1µlLipo

Table 5: Protocol for TRD and TRDL mediated transfections.

2.2.1.3 Luciferase reporter assay:

The detection of luciferase activity in the cells transfected with reporter vectors containing the firefly gene was performed with the luciferase reporter assay kit (Promega). The luciferase assay is based on the enzyme-catalyzed chemiluminescence. Luciferin present in the luciferase assay reagent is oxidized by luciferase in the presence of ATP, air oxygen and magnesium ions. This reaction produces light with a wavelength of 562 nm that can be measured by a luminometer. After washing twice with 1 x PBS, the transfected cells were incubated for 15 m in 70 µl of 1x lysis buffer on a shaker. Following a cycle of freeze thawing luciferase measurements were performed. For measurement of firefly luciferase activity, 20 µl of the lysate were mixed in white and flat bottom 96-well plates containing 100 µl luciferase assay reagent, which was freshly prepared by mixing substrate and the luciferase assay buffer. The luminescence was measured in luminometer for firefly luciferase activity.

5 x lysis buffer (pH 7.8)	Volume	Final concentration
1M Tris	25 ml	125 mM
200 mM EDTA	10 ml	10 mM
500 mM DTT	4 ml	10 mM
85 % Glycerol	115 ml	50 %
Triton X-100	10 ml	5 %
H_2O	to 200 ml	

2.2.1.4 MTT cell proliferation assay:

MTT [3-(4, 5-dimethylthiazol-2-yl)-2, 5-diphenyltetrazolium bromide] assay was first described by Mosmann in 1983. It is based on the ability of a mitochondrial dehydrogenase enzyme from viable cells to cleave the tetrazolium rings of the pale yellow MTT and form dark blue formazan crystals which are largely impermeable to cell membranes, thus resulting in their accumulation within healthy cells. The number of surviving cells is directly proportional to the level of the formazan product created. The color can then be quantified using a colorimetric assay.

About 5000 cells/well were plated in a 96-well plate. The cells were transfected with TRDL vectors. The following morning the medium was replaced by 100µl fresh culture medium and the cells were incubated for 2 h at $37^{o}C$. 10µl of MTT reagent was added in each well and incubated for 1-2 h in dark. The color change was carefully monitored. The absorbance was measured at 570 nm. A triplicate of untreated cells was taken as blank. The average absorbance of blank should range between 0.1-0.2. The sample absorbance was calculated as:

Sample absorbance = Absorbance measured – Average absorbance of blank.

2.2.1.5 Cyto-toxicity assay:

The cyto-toxicity measurement was performed with the CytoTox-ONE^{TM} homogeneous membrane integrity assay. CytoTox-ONE^{TM} is a rapid, fluorescent measure of the release of lactate dehydrogenase (LDH) from cells with a damaged membrane. LDH released into the culture medium is measured with a 10 m coupled enzymatic assay that results in the conversion of resazurin into florescent resorufin. The reagent mix does not damage the cells and therefore measurements can be performed in wells containing a mixed population of viable and damaged cells.
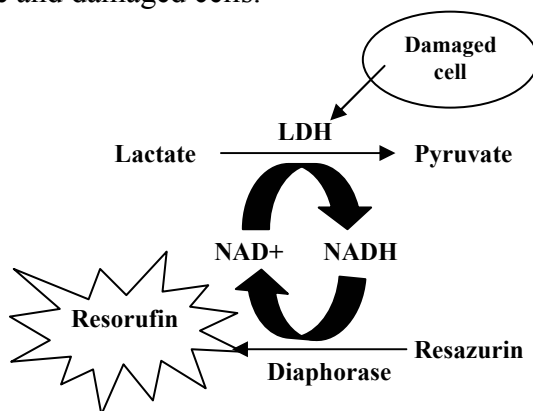
Figure 6: **Principle of CytoTox-ONE^{TM} homogeneous membrane integrity assay.** Release of LDH from damaged cells is measured by supplying lactate, NAD$^+$ and resazurin as substrates in the presence of diaphorase. Generation of the fluorescent resorufin product is proportional to the amount of LDH.

2.5×10^4 cells/well were plated in a 96-well plate. The cells were incubated with test compounds (DNA+OptiMEM, TRD+OptiMEM, TRDL+OptiMEM and DL+OptiMEM) for 4 h at 37°C. Following this, the test compounds were removed and 100µl culture medium was added. Cells were cultured overnight at 37°C. The assay plate was removed from 37°C incubator and equilibrated to 22°C for 20 m. 100µl CytoTox reagent was added in each well. The plate for incubated at room temperature for 10 m. Following this incubation 50µl stop solution was added. The plate was incubated at room temperature on a shaker for 10 s and the florescence was measured with an Ex λ - 560nm and Em λ - 590nm. Triplicate wells with out cells to serve as negative control, in order to determine background florescence was employed. Untreated cell control and Maximum LDH release controls were also performed in triplicates, with cells untreated with test compounds and cells lysed with 2µl lysis solution respectively.

The average florescence values of the culture medium background were subtracted from the experimental values. The percent cyto-toxicity was then calculated employing the formula:

% Cyto-toxicity = 100 × (Experimental – Culture medium background) ÷ (Maximum LDH release – Culture medium background)

2.2.1.6 Analysis of DNA uptake:

A 400bp *Fam*-CMV fragment was amplified from Pgl3CMV. About 5×10^5 cells/well were plated in a 6-well plate and cultured overnight. The cells were transfected in duplicates with *Fam*-CMV employing TRDL and DL vectors. Following this the cells were used for DNA isolation.

Fam-CMV isolation from cell lysate:

Following transfections, the cells were lysed with 100µl lysis buffer and the lysate was PCR column purified. The eluent (100µl) was used for gene scan analysis of Cellular DNA.

Fam-CMV isolation from Nucleus:

Following transfections, the cells were subjected to nuclear isolation. The cells were washed with PBS for 2 times. The cells were scraped with 500µl PBS and centrifuged at 400g for 5 m at 4°C. The supernatant was discarded and the pellet was re-suspended in 2000µl buffer I (10mM Tris HCl, 1.5mM $MgCl_2.6H_2O$ and 10mM KCl, pH-7.8) and incubated on ice for 10 m. The cells were homogenized for 10 s at 3000U. The homogenate was checked under microscope for nuclear isolation. Confirming nuclear release, the homogenate was centrifuged at 4500g for 5 m at 4°C. The pellet was re-suspended in 1000µl buffer II (420mM KCl, 20mM Tris HCl, 1.5mM $MgCl_2.6H_2O$ and 20% Glycerol, pH-7.8). The suspension was centrifuged at 10000g for 30 m at 4°C. The supernatant containing the nuclear extracts were PCR column purified. The eluent (100µl) was used for gene scan analysis of nuclear DNA.

Gene Scan analysis:

Samples for gene scan were prepared by mixing 1µl of each sample (Cell, Nucleus and known amounts of *Fam*-CMV ranging from 0.5ng to 24ng) with 0.5µl of Genescan 500 TAMRA size standard (PE Applied Biosystems) and 18.5µl of template suppression reagent (TSR). The samples were denatured at 99°C for 10 m and cooled on ice for 5 m. The samples were run in an ABI prism 310 genetic analyzer, under the conditions: Module- GS STR POP4 (1ml) C, Injection seconds- 5, Injection KV- 15, Run KV- 15 Run °C- 60, Run time- 30 m. The gene scan software was used to size and quantify the DNA fragments.
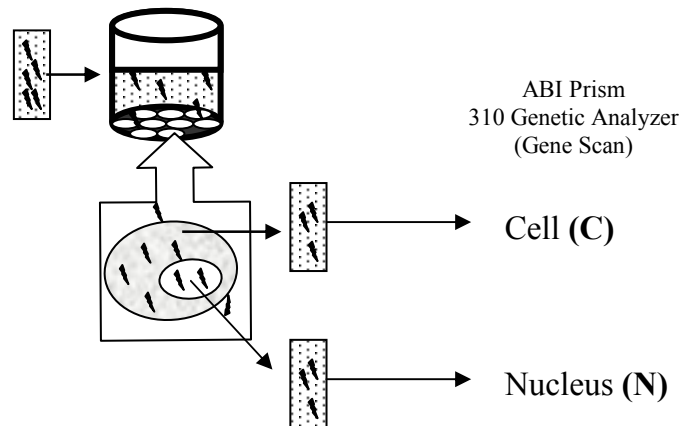

Figure 7: **Principle of Analysis of DNA uptake.**

2.2.1.7 Immunostaining and confocal imaging:

TatRGD and caveolin-1 co-localization:

About 0.5×10^5 cells/well (A549) were plated in 8-well permanox chamber slides (Lab-Tek, Naperville, IL, USA) pre-coated with 300 μl fibronectine (20 μg/ml). After overnight culturing, A549 cells were transfected with 400 bp DNA fragment (CMV), employing TRDL vector system. The cells were fixed at different time points, for 2 h at room temperature with PFA (1 ml 4% paraformaldehyde, 0.4 ml 10x PBS and 2.6 ml H_2O). The cells were washed 3 times with 1x PBS and unspecific binding of the primary antibody was blocked for 1 h with 5% BSA and 5% normal goat serum in 1x PBS. Following this, the cells were washed and incubated overnight in a humid chamber with polyclonal rabbit anti-caveolin-1 primary antibody (1:400) (Santa Cruz, Santa Cruz, USA). The cells were washed and incubated for 1 h with Cy5-conjugated donkey anti-rabbit IgG secondary antibody (1:200) (Dianova, Hamburg, Germany). Then, the cells were washed and incubated for 1 h with Cy3 conjugated streptavidin (1:5000) (Dianova, Hamburg, Germany) for labeling biotin-TatRGD. The slides were mounted with a coverslip and analyzed by laser-scanning confocal fluorescence microscopy for TR and caveolin-1 co-localization.

Cellular internalization of TatRGD:

The cells were cultured, transfected and fixed as mentioned above. Blocking and permeabilization was performed with 10% horse serum, 0.5% Tween 20, 0.1% BSA in 1x PBS for 1 h. Permeabilization ensures that the secondary reagent (Cy3-conjugated streptavidin) enters the cells and labels the biotin-TatRGD which can be analysed by confocal microscopy for the cellular internalization of TR.

Intracellular Localization of DNA:

Cells (A549 or SMC$_{PA}$) were transfected with *Fam*-labeled DNA fragment (*Fam*-CMV), employing TRDL vector system and fixed at different time points with PFA. The cells were washed and blocked with 5% BSA, 5% normal goat serum in 1x PBS for 1 h. Following this, the cells were washed and incubated overnight in a humid chamber with polyclonal rabbit anti-caveolin-1 primary antibody (1:400) (Santa Cruz, Santa Cruz, USA). Then, the cells were washed and incubated for 1 h with Cy3-conjugated donkey anti-rabbit IgG secondary antibody (1:400) (Dianova, Hamburg, Germany). Afterwards,

the cells were incubated sequentially for 10 m with WGA-633 membrane dye (Wheat germ agglutinin Alexa Fluor 663-conjugated, Molecular Probes: W-21404, 1:100) and TO-PRO-3 nuclear stain (Molecular Probes, 1:800). The cells were mounted with a coverslip and analyzed by laser-scanning confocal fluorescence microscopy for the intracellular localization of *Fam*-labeled DNA.

The following laser lines were employed to detect the corresponding flurophores: *Fam* was detected using the 488nm laser line, Cy-3 was detected using the 543nm laser line and Cy-5, WGA-633 and TO-PRO-3 were detected using the 633nm laser line, all with appropriate detection bandwidths for each fluorophore. Sequential scanning was performed to prevent bleed through into adjacent detection channels.

2.2.2 Molecular biology methods:

2.2.2.1 Cloning of DNA fragments into plasmids:

For cloning of the full length RELMβ cDNA we performed RT-PCR using RNA extracts from human lung tissue with primers derived from human RELMβ cDNA sequence (Acc. No.: AF323084): PHIMF-f and M-HIMF-f. The purified PCR product was ligated into pGEM-T-easy plasmid (Promega) and positive clones were sequenced. Inserts from pGEM-T-easy plasmid were amplified by PCR for sub-cloning into pCMV-HA expression plasmid (Clontech, Paolo Alto, USA) using the following primers: HIMF-kozak-kpn1 and HIMF-HA-TGA-xho1. The forward primer contained a *Kozak* sequence as an optimized translation start and the reverse primer carried a hemeagglutinin A (HA) tag in frame at the C-terminus. Primer sequences are mentioned in the materials section.

2.2.2.2 Polymerase chain reaction:

In the polymerase chain reaction (PCR), the DNA sequence of interest undergoes repeated doubling in an exponential fashion. Two synthetic oligonucleotides (primers) complementary to the 3' end of the target DNA (template) were added at high concentrations. The reaction additionally involves the use of four deoxyribonucleotide triphosphates (dNTPs) and a heat-stable DNA polymerase. Each cycle consists of three reactions that take place under different temperatures. First, the double-stranded DNA is denatured (95°C) into its two single strands, which functions as templates for the synthesis of new DNA. Second, the reaction is cooled (50-60°C) to allow the annealing

of primers to the complementary DNA strands. Third, DNA polymerase extends both DNA strands at 72°C starting from the primers.

PCR reaction	**(per 25 µl)**
Template DNA	10 ng
Forward primer	10 pmol
Reverse primer	10 pmol
40 mM dNTP mix	0.5 µl
10 x PCR buffer	2.5 µl
HotstarTaq polymerase	2.5 U
H_2O	Made to 25 µl

The PCR was performed in a thermal-cycler programmed as follows:

Activation of HotstarTaq		95^oC	15 m
Denaturation		94^oC	20 s
Annealing		Table 6	30 s
Extension		72^oC	Table 6
Cycles	35 to 40		
Final extension		72^oC	10 m

After the amplification, PCR products (10 µl) were electrophoretically analyzed in a 1% agarose gel with 0.2 µg /100 ml ethidium bromide and purified if required.

DNA fragment	**Annealing temperature**	**Extension time**
Fam-CMV / CMV(400bp)	60^oC	25 s
Full length HIMF	63.5^oC	20 s
HIMF (200bp)	52^oC	30 s
HPRT	52^oC	30 s

Table 6: List of annealing temperatures and extension times for PCR.

2.2.2.3 DNA electrophoresis and purification from agarose gel:

The DNA samples were mixed with loading buffer and loaded onto the 1% agarose gel. The electrophoresis was performed for 45-60 m with 5 V/cm. The negatively charged DNA migrated from the cathode (-) to the anode (+). To visualize DNA, the gel was treated with ethidium bromide (0.5 µg/ml), which intercalated between the bases of DNA double strands forming a complex, fluorescent under UV light. The size of DNA fragments was determined by a DNA molecular weight standard.

Loading buffer	**Final concentration**
Bromophenol blue	0.01 g /100 ml (0.01%)
Glycerol	40 ml /100 ml (40%)
10 x TAE buffer	10 ml / 100 ml (1x)

The corresponding DNA fragment was excised from the gel and purified with the QIAEX II kit (Qiagen). Three volumes of binding and solubilization buffer (QX1) and 10 µl QIAEX II solution were added to 1 volume of gel. For effective DNA binding, the solution was incubated at 50°C for 10 m with occasional mixing. After centrifugation at 20,800 g for 30 s, the pellet was washed once with QX1 buffer and once with PE buffer. After aspirating the washing buffer, the pellet was completely dried at room temperature (for about 15 m). Then, the pellet was re-suspended in 20 µl H_2O and incubated for 5 m at room temperature. After centrifugation at 20,800 g for 1 m, the supernatant containing the DNA fragments was collected into a fresh tube.

2.2.2.4 Direct PCR product purification (column purification):

The PCR products were purified with the Qiaquick PCR purification kit (Qiagen). Binding buffer (BP) was added to PCR solution at the ratio of 5:1 v/v, respectively. The solution was loaded onto the Qiaquick column to which the DNA binds. After centrifugation at 20,800 g for 30 s, the column was washed with washing buffer and completely dried by centrifuging at 20,800 g for 1 m. Then, the fragment was eluted in 50µl H_2O by centrifugation at 20,800 g for 1 m into a fresh tube.

2.2.2.5 Restriction digestion:

The DNA fragments (Plasmid or PCR products) were restriction digested using the following protocol. The mixtures were incubated at temperatures for maximum activity of the specific enzymes.

Total reaction volume	(per 10 μl)
Plasmid / PCR product	3 μg / 8 μl
Enzyme	1μl
10 x buffer	1μl

2.2.2.6 Ligation:

The purified DNA fragments were ligated into the linearized plasmids by T4 ligase. The ligation reaction was incubated overnight at 16°C and then transformed in the competent *E.Coli* cells.

Total reaction volume	(per 10 μl)
DNA fragment	100 ng
Linearized plasmid	50 ng
10 x ligase buffer	1μl
T4 DNA ligase	1μl
H_2O	Up to 10 μl

2.2.2.7 Preparation of competent *E.coli* :

A single bacterial colony from the *E.Coli* TOP10 glycerol culture was cultured in 5 ml LB medium at 37°C overnight. Following day, the bacterial suspension was diluted into 500 ml LB medium and cultured till the OD at 550 nm became 0.3-0.4 (about 3-6 h). The suspension was centrifuged at 4°C, 5000 *g* for 15 m. The pellet was re-suspended in 100 ml ($1/5^{th}$ vol) ice-cold 50mM $CaCl_2$ and kept on ice for 5 m. The cells were again centrifuged at 4°C, 5000 *g* for 15 m. The pellet was re-suspended in 25 ml ($1/20^{th}$ vol). The cells were again centrifuged at 4°C, 5000 *g* for 15 m and pellet was re-suspended in 5 ml of 50 mM $CaCl_2$ in 20% glycerol. Suspension was divided in 50 μl aliquots and

stored at -70°C. The competence of the bacterial cells was checked by the transformation of an ampicillin resistant plasmid.

Luria Bertani medium (LB)	Final concentration
Tryptone	10 g/l
Yeast extract	5 g/l
NaCl	10 g/l
pH	7.3

2.2.2.8 Transformation of *E.coli*:

The transformation of *E.coli* was performed by heat shock method. The ligation mixture or the plasmid DNA was gently mixed with one aliquot of the competent cells and incubated at 4°C for 30 m. Then the mixture was heated to 42°C for 2 min and cooling on ice immediately. Thereafter, the bacterial cells were cultured in 200 µl SOC medium without antibiotics at 37°C for 1h. An aliquot of 100 µl was spread over an ampicillin containing agar dish and incubated overnight at 37°C.

SOC medium	Final concentration
Tryptone	2 %
Yeast extract	0.5 %
NaCl	10 mM
KCl	2.5 mM
$MgCl_2$	10 mM
$MgSO_4$	10 mM
Glucose	20 mM
pH	7.3

Ampicillin agar dishes:

For preparing the agar plates, 500 ml LB medium containing 7.5g bactoagar was autoclaved. After cooling to 50°C, 500 µl ampicillin stock solution (final concentration 10% w/v) was added, mixed and 20 ml of the solution was poured into each sterile

culture dish. The dishes were left for solidifying at room temperature overnight and then stored at 4°C in the dark.

Ampicillin stock solution: 0.1 g/ml

Colony PCR from bacterial culture:

The bacterial colonies transformed with a ligation mixture or with a plasmid, were picked and cultured in 5 ml LB medium with ampicillin (100µg/ml) at 37°C overnight. 10 µl of each bacterial culture was re-suspended in 90 µl of H_2O, heated at 95°C for 10 m and cooled on ice. 1 µl of this suspension was used as template in setting the 25 µl PCR reaction using the primers specific for the fragment in question.

2.2.2.9 Isolation of plasmid DNA:

The maxi-preparation of plasmid DNA was performed with Nucleobond AX500 Maxi-prep Kit according to manufacturer's descriptions. The transformed *E.Coli* TOP10 cells were cultured in 200 ml LB medium to a density of about 109 per ml (OD at 600 nm of 1-1.5). The cells were pelleted by centrifugation at 4°C, 5860 *g* (6000 rpm, GSA rotor) for 30 m. The pellet was re-suspended in 10 ml of buffer S1, which contained 100 µg/ml of RNase. Then 10 ml of buffer S2 (with NaOH and SDS for bacterial lysis) was added and mixed gently 4-6 times (the mixture was not vortexed to avoid shearing of genomic DNA). After 5 m incubation at RT (longer incubation could lead to irreversible denaturation of plasmid DNA), 10 ml of buffer E3 was added to neutralize the solution. The solution was filtered using the paper filters provided in the kit. The filtrate was carefully applied to the column, which was equilibrated with 6 ml of buffer N2. When the lysate has been completely run by gravity flow, the column was washed twice with 18 ml of buffer N3 to remove single stranded DNA, RNA and all other impurities such as proteins, metabolites, polysaccharides and NTPs. Afterwards, the double stranded plasmid DNA was eluted with 15 ml of buffer N5 and precipitated by adding 10.5 ml of isopropanol. Plasmid DNA was pelleted by centrifugation at 4°C, 27000 *g* (5000 rpm, SS34 rotor) for 30 m. The DNA pellet was washed with 70% ethanol, to remove salts, air-dried for 30 m and dissolved in 500 µl H_2O.

To determine the DNA concentration and the presence of protein in the probes, the OD at 260 nm (DNA) and 280 nm (protein) was measured. The prepared plasmids were checked by restriction analysis as described above.

Buffers used in maxi preparation:

Buffer S1	**Final concentration**
Tris-HCl	50 mM
EDTA	10 mM
RNase A	100 mg/ml
pH	8.0

S1 with Rnase A was stored at 4°C

Buffer S2	**Final concentration**
NaOH	200 mM
SDS	1 %

Buffer S3	**Final concentration**
Potassium acetate pH 5.1	2.8 M

Buffer N2	**Final concentration**
Tris	100 mM
Ethanol	15 %
KCl	900 mM
Triton X-100	0.15 %
pH (adjusted with H_3PO_4)	6.3

Buffer N3	**Final concentration**
Tris	100 mM
Ethanol	15 %
KCl	1.15 M
pH (adjusted with H_3PO_4)	6.3

Buffer N5	**Final concentration**
Tris	100 mM
Ethanol	15 %

KCl	1.0 M
pH (adjusted with H_3PO_4)	8.5

2.2.1.10 Sequencing of plasmids:

The sequencing was performed by a "Big-dye terminator cycle sequencing" method following the manufacturer's protocol (Perkin Elmer). In this method, the premix solution contains four dideoxynucleotides (ddNTP, each labeled with a different fluorescent dye), unlabeled deoxynucleotides (dNTP) and a temperature resistant DNA polymerase. The template plasmid and the gene specific primer (forward or reverse) were added to the reaction mixture. During the PCR reaction, the synthesized single strand DNA would be stopped randomly with the incorporation of ddNTP. Thus, DNA fragments of different size were labeled at their 3´-ends with base specific fluorescent dyes, which could be analyzed with the DNA sequencer (ABI, model 310 Genetic Analyzer)

Sequencing reaction	Volume	Final concentration
Plasmid	x µl	1µg/probe
Primer (2.5 pmol/µl)	2 µl	5 pmol/probe
Premix	2 µl	
H_2O	to 10 µl	

The sequence reaction was performed under following conditions: denaturation at 96°C for 10 s, primer annealing at 50°C for 5 s, extension at 60°C for 4 m. After the sequencing reaction the solution was cooled at 4°C and purified as follows:

10 µl 3 M NaAc, pH 5.2, 80 µl H_2O and 250 µl 95% ethanol (RT) was added to the sequencing mixture and centrifuged for 20 m at 15,800 *g* (14,000 rpm, table centrifuge). The pellet was washed with 250 µl of 70% ethanol, centrifuged for 10 m, air-dried and re-suspended in 20 µl of Template Suppression Reagent (TSR). Then, the probe was loaded on the capillary sequencer using the performance-optimized polymer 6 (POP6). The fluorescent signal was identified by the detector system of the DNA sequencer and quantified.

2.2.1.11 RNA isolation from cultured cells:

The RNA was extracted from cells using guanidine thiocyanate-acid phenol (RNAzol-B, WAK-Chemie, Germany). RNAzol-B is a complete and ready-to-use reagent for isolation of total RNA from samples of human, animal, plant, bacterial and viral origin. A biological sample was lysed in RNAzol-B and the lysate was separated into aqueous and organic phase by the addition of chloroform. The subsequent centrifugation efficiently removes DNA and proteins from the aqueous phase containing RNA. The non-degraded, pure RNA is obtained from the aqueous phase by the isopropanol precipitation. The RNA pellet was washing with ethanol and solubilized in an appropriate solution. Cultured cells (3×10^5 cells in 6 well culture dishes) were washed with 1 x PBS, and scraped in 400 µl RNAzol-B buffer with a disposable cell scraper. The cell lysate was homogenized by pipetting up and down, and then transferred into a 2 ml Eppendorf cup. Thereafter, 80 µl of chloroform was added with gentle mixing. The solution was incubated on ice for 15 m and centrifuged at 10000 g, 4°C for 20 m. The RNA-containing upper phase was collected in a new 2 ml Eppendorf cup. The RNA was precipitated by addition of 0.2 ml isopropanol and centrifuged at 10,000 g, 4°C for 10 m, the RNA pellet was washed once with 200 µl 70% ethanol. The purified RNA was centrifuged again for 10 m at 10,000.g and dried in an air at room temperature for 10 m. Finally, the pellet was dissolved in 30 µl H_2O. After measuring the RNA concentration the samples were stored at -70°C.

To determine the concentration and purity of the RNA, the extinction at 260 nm and 280 nm was measured. An OD of 1 at 260 nm corresponds to 40 µg RNA/ml. The ratio of the OD at 260 nm and at 280 nm is a measure of RNA purity. In a protein-free solution the ratio OD260/OD280 is 2. Due to protein contaminations this coefficient is usually lower. In our experiments it was between 1.6 and 2.

2.2.1.12 Preparation of cDNA from RNA probes:

For the preparation of cDNA, 1µg RNA per sample was used. RNA was copied to cDNA using reverse transcriptase (MMLV-RT) (Invitrogen, Carlsbad, USA) with $p(dT)_{15}$ primers. For the negative controls, MMLV-RT was omitted.

RNA (1 µg /10 µl) was denatured at $65^{o}C$ for 5 m followed by rapid cooling and addition of 10 µl master mix; containing the following:

5x first strand buffer	4 µl
0.1 M DTT	2 µl
10mM dNTP mix	1 µl
$p(dT)_{15}$ primer	1 µl
RNase inhibitor	1 µl
MMLV-RT (200U/1 µl)	1 µl

The denatured RNA mixed with master solution was then subjected for cDNA synthesis by incubating at $39^{o}C$ for 1 h followed by inactivation of enzymes at $96^{0}C$ for 2 m. (DNase treatment prior to RNA denaturation was performed to some samples where genomic DNA contamination was encountered. DNase was added at a concentration of 10 units/µg RNA and incubated at $37^{0}C$ for 30 m. Following this RNA denaturation was performed at $65^{0}C$. At this temperature the DNase is also deactivated).

2.2.1.13 Protin preparation and Western blot analysis:

Total protein isolation from the cultured cells:

The cultured cells were washed with ice-cold 1 x PBS and lysed using 1x Lamelli buffer (NuPAGE LDS sample buffer- 4x) was diluted to 1x with 2% mercaptoethanol. The mixture was incubated at 95°C for 5 m before adding to the cells).

PolyAcrylamide Gel Electrophoresis of protein (SDS-PAGE):

In SDS-PAGE the denatured polypeptides bind to SDS and become negatively charged. The amount of SDS bound is always proportional to the molecular weight of the polypeptide and is independent of its sequence. Therefore, SDS-polypeptide complexes migrate through polyacrylamide gels in accordance with the size of the polypeptide. By using markers of known molecular weight, it is therefore possible to estimate the

molecular weight of the polypeptide chains. Protein sample from cell lysate and supernatant was denatured by heating to 95°C for 5 min in 1 x loading buffer, and then cooled on ice immediately. The samples were collected by brief centrifugation and then loaded on ready to use Novex 16% Tricine gel. The electrophoresis was performed at constant volt at 200 V and the gel was run till the bromophenol blue reached the bottom of the resolving gel (for about 1 h). The gel was then used for Western-blot analysis

Electro blotting of immobilized proteins:

The separated proteins on the SDS-polyacrylamide gel were electrically transferred to a polyvinylidene fluoride (PVDF) membrane by electro blotting. The PVDF membrane was activated by methanol before use. The transfer equipment was prepared in the following way: two layers of 3mm Whatmann filter paper washed with transfer buffer followed by activated PVDF membrane washed with transfer buffer were placed onto the electro blotting chamber. On the PVDF membrane, the gel and the other two layers of filter paper washed with transfer buffer were placed. The cathode and anode from the power supply were connected with the electro-blotting chamber. Electro blotting was performed at constant current ($2mA / cm^2$) for approximately 90 min.

Transfer Buffer (pH = 8.3)	**Final concentration**
Tris	25 mM
Glycine	192 mM
Methanol	20 %
SDS	0.01 %

Immunological detection of immobilized proteins:

The membrane was blocked with 0.25% gelatin in 1 x NET buffer at room temperature for 1h followed by incubation with primary antibody at 4°C overnight. After washing with 1 x NET for three times (10 m each), the membrane was incubated with the respective secondary antibody at room temperature for 2 h followed by three times washing with 1 x NET buffer. Membrane was then incubated with biotin-streptavidin-horseradish peroxidase complex for 1 h followed by three times washing with 1 x NET buffer. The protein bands were detected by ECL (Enhanced Chemi-luminescence)

treatment, followed by exposure of the membrane in fluorChem 8900 chemi-luminescence imager.

10 x NET buffer	Final concentration
NaCl	1.5 mM
EDTA (pH = 8.0)	50 mM
Tris	500 mM
Triton X-100	0.5 %

2.2.1.14 Conjugate peptide TatRGD synthesis:

The biotinylated TatRGD (TR) peptide consisting of the truncated Tat domain at the N-terminus and the domain with an RGD motif at the C- terminus had the following sequence: (Biotin–GMLGISYGRKKRRQRRRPPQT GGCRGDMFGC). This peptide was synthesized (Peptide- Synthesizer 432A, Applied Biosystems Fmoc-chemistry) and labeled at the N-terminus with biotin. After deprotection it was purified by HPLC. The two cysteine residues were oxidized by air-oxygen and a second HPLC purification was performed.
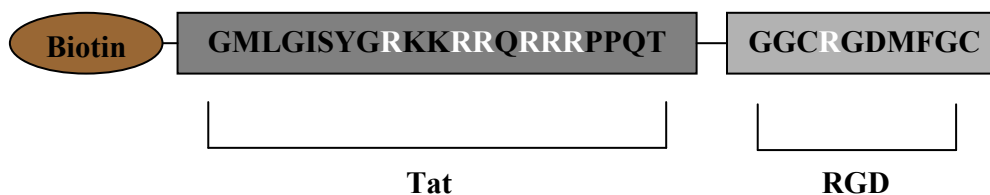
Figure 8: **TatRGD conjugated peptide.** Biotinylated TatRGD peptide, contains 21mer Tat (dark gray) and 10mer RGD (light gray) sequence. The peptide has in total 7 Arginine residues (white), which contribute to the net positive charge of the peptide.

2.2.1.15 Particle size measurements:

Particle size measurements were performed using the Zeta sizer, which is based on the principle of light scattering. DNA (1µg) was mixed with different concentrations of TatRGD (2, 4, 6, 12.5, 25µg) in HBS (pH-7.4), in order to obtain TRD mixture. The mixtures were incubated for 15 m and measured for particle size using a zeta sizer. TRDL complexes were obtained by adding 2µl lipofectamine to the TRD mixture and

incubating for 15 m at room temperature. The TRDL mixtures were then measured for particle size using zeta sizer.

2.2.1.16 Sephadex Column packing and separation:

Sephadex G-100 (Pharmacia Biotech, Uppsala, Sweden) was employed for separation. To pre-swell the gel, 250 ml ultrafiltered water was added to 3g Sephadex G-100. The gel was autoclaved and incubated overnight at room temperature. When the pre-swollen gel settled at the bottom of the bottle, the slurry supernatant was decanted to remove the gel fines. Additional 200 ml ultrafiltered water was added to prevent gel drying.

Column packing:

23 cm Glass chromatographic columns (Glass pasture pipettes, VWR International), with 10cm packing volume, were employed. The bottom of the column was blocked with cotton wool and clamped vertically with the separation nozzle facing down. Before packing the column with Sephadex G-100, 500µl HBS was added to the column in order to ensure free flowing. The pre-swollen gel was mixed to obtain homogeneous slurry. The gel slurry was then added to the column avoiding any air bubble formation. All columns were packed to 5 cm height. Equilibration of the columns was performed with HBS buffer.

Sample separation:

Following the equilibration of the column with HBS buffer, 75µl of the sample (1µg DNA + 2, 4, 6, 12.5 and 25 µg TR for each sample. The volume was made to 75µl with HBS and samples incubated for 15 m) was loaded into the column. Additional 500µl HBS was added and the eluents were collected in 10 batches with 6 drops in each batch. Control samples without column elution, were prepared with 1µg DNA + 2, 4, 6, 12.5 and 25 µg TR for each sample. The volume was made to 75µl with HBS and samples incubated for 15 m. The eluents collected from the sephadex columns and the corresponding control samples, were vacuum dried and re-suspended with 10µl 20x SSC (3M Sodium Chloride and 0.3M Sodium Citrate, pH- 7.0) for dot-blot analysis.

2.2.1.17 Dot-blot analysis:

The samples obtained from the Sephadex column separation, were dotted on a nylon membrane and the membrane was baked at 60°C for 5 m. The 1x blocking buffer was prepared by diluting the 10x stock solution (Blocking reagent for nucleic acid hybridization and detection (Roche), was dissolved in maleic acid buffer to a final concentration of 10% w/v with heating and shaking. The 10x stock solution was autoclaved and stored at 4° C) with maleic acid buffer (100mM maleic acid and 150mM NaCl, Ph-7.5). The membrane was blocked with 1x blocking buffer for 1 h. The membrane was then washed for 3 times with 50mM Tris and 0.1% Tween 20, pH – 7.4. The membrane was then incubated with avidin peroxidase (1:5000) for 1 h, followed by 3x washing. The membrane was developed with Diamino benzydene (DAB) substrate (4mg DAB, 4.5ml 50mM Tris, 0.5ml $NiCl_2$, 5μl H_2O_2). Quantification of the dots was performed by employing densitometric software (fluorChem 8900 chemi-luminescence imager).

In order to obtain the total signal intensity caused by different concentrations of TR the standard curve was plotted, by dotting TRD (containing 1μg DNA + 2, 4, 6, 12.5 or 25μg TR) directly (with out column separation) on the membrane and backing at 60^oC. The dots were developed and quantified as mentioned above and used to plot the standard curve.

Note: Since TR and not the plasmid DNA, is biotin conjugated the color development with avidin peroxidase incubation and subsequent development with DAB, is due to TR. While TR does not bind to nylon membrane by it self (observed by dotting TR alone on the membrane, gave no colored dots). It requires binding with DNA for successful colored dotting on the blot. Backing however facilitates residual amounts of TR un-complexed with DNA also to bind to the membrane. Hence the standard curve was plotted to obtain the total signal intensity caused by different concentrations of TR.

2.3 Security Measures:

All the operations with genetically modified organisms and plasmid DNA were performed according to the ''Gentechnikgesetz of 1990'' and to the rules prescribed by the ''Gentechnik-Sicherheitsverordnung of 1990''. Materials contaminated with bacterial cells were autoclaved. The chemicals like formaldehyde, DEPC, phenol and ethidium bromide are carcinogenic and were carefully managed and disposed.
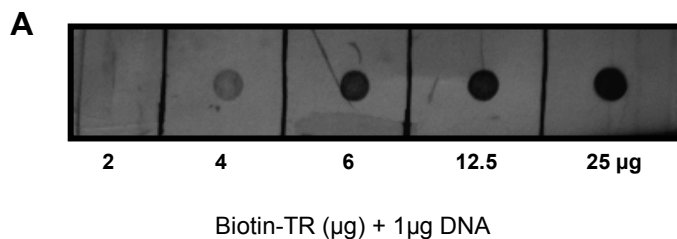
3. Results:

3.1 Synthetic peptide TatRGD mediated gene transfer in lung cells:

3.1.1 TatRGD and DNA Binding Analysis:

We performed binding experiments between TatRGD (TR) and DNA, to determine an appropriate concentration ratio of TR and DNA. Firstly, the standard curve was obtained by dotting biotin-TRD (containing 1µg DNA mixed with 2, 4, 6, 12.5 or 25µg TR) directly (with out column separation) on the membrane and backing at 60°C. The dots were developed, quantified and used to obtain the standard curve. The intensity of the dots obtained were directly proportional to the amount of TR employed *(figure 9-A)*.

TatRGD-DNA (TRD) complexes were prepared by mixing 1µg DNA with corresponding concentrations (2, 4, 6, 12.5, 25µg) of biotin-TR in HBS at physiological pH. These TRD mixtures were passed through Sephadex G-100 columns and eluted in 10 fractions containing 6 drops each. When biotin-TR alone was passed through the column no dots were found on the blotting membrane until 12 fractions (no color appeared on the blots). Hence the TRD complexes were eluted in 10 fractions for each sample. The eluents from Sephadex G-100 seperation were dot-blotted and quantified as mentioned in the methods section. When TRD mixtures were passed through the Sephadex G-100 columns, only stable TRD complexes formed were assumed to be eluted in the first 12 fractions. The results obtained were in correspondence with this. Colored dots were seen only in the 5th and 6th fractions of elution *(figure 9-B)*. By fitting these values in the standard curve the approximate amounts of TR bound per µg DNA was obtained.

The binding curve was then plotted with the input amount of TR on the x-coordinate and the amount of TR bound to 1µg DNA on the y-coordinate *(figure 9-C)*. Figure 9-B and C suggests that, a minimum of 4µg TR is required per µg DNA to obtain TRD complexes. Binding saturated at approximately 12 µg TR per µg DNA.

Biotin-TR (µg) + 1µg DNA

B

Dot 5

Dot 6

2   4   6   12.5   25 µg

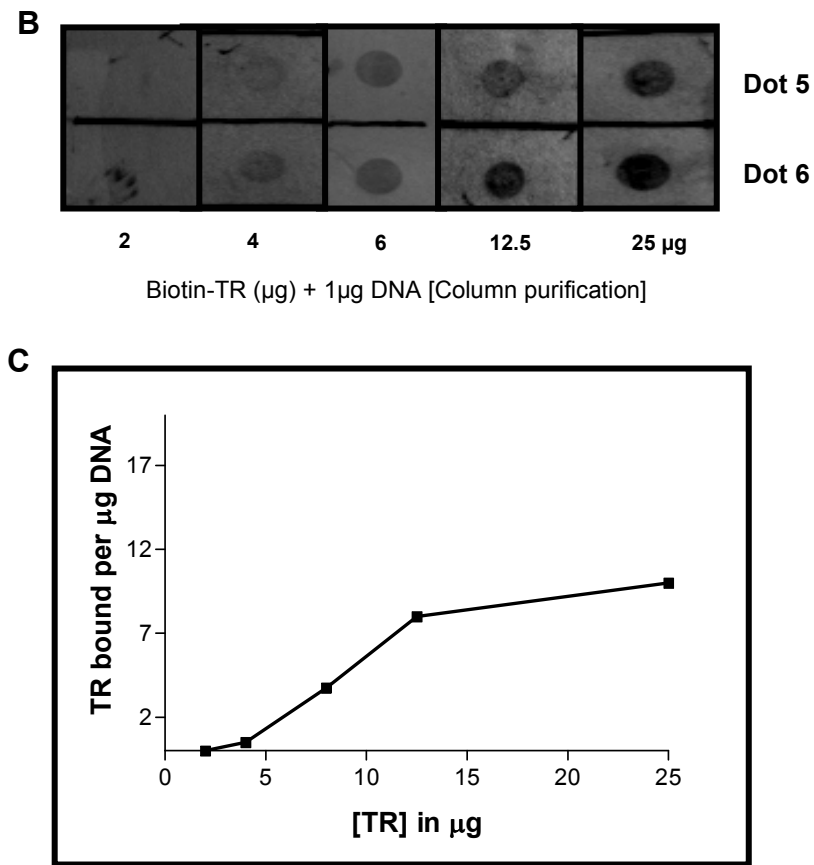Biotin-TR (µg) + 1µg DNA [Column purification]

C

Figure 9: TRD binding analysis. Dot blots obtained by direct application of TRD complexes were used for obtaining the standard curve (A). Dot blots were obtained by dotting eluents from column separation (B). Binding curve suggested the amount of TR bound /µg DNA (C).

3.1.2 Particle size measurement:

Since the size of the particle is one of the important criterions for its cellular internalization, particle size measurements were performed for TRD and TRDL complexes. When TatRGD and DNA were alone measured, the average diameter was beyond the range of the instrument (i.e.) >6µm. But, when TatRGD was mixed with DNA, the average diameter of the TRD complexes reduced ranging between 1µm and 2.5µm. TRD complexes with lower TR concentrations formed particles with smaller diameters. Further reduction in the average diameter was observed when lipofectamine was added to the TRD mixtures. This suggests that, addition of lipofectamine to TRD, results in further compaction of the particles which aids in better internalization.
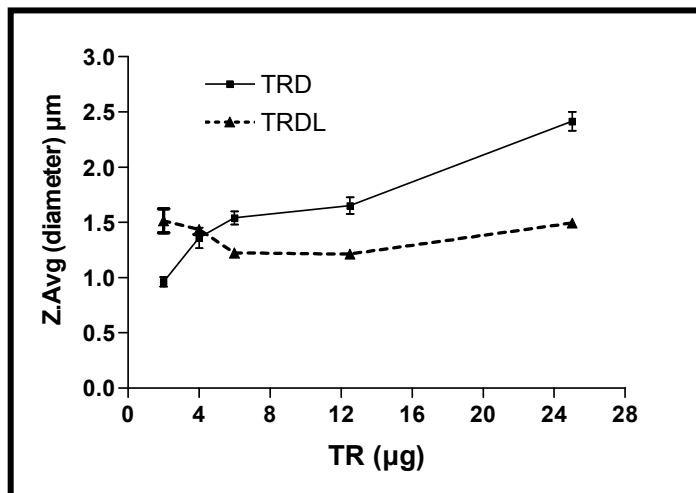
Figure 10: **Particle size measurements.** Measurement of particle sizes of different amount of TR added to DNA (TRD) or different amounts of TR added to DNA complexed with Lipofectamin (TRDL). Z. Avg represents the average size.

3.1.3 Dose response:

To investigate the applicability of TatRGD as a transfection agent, the effect of different TR amounts per µg DNA on transfection efficiency was studied employing luciferase reporter gene.

In case of A549 cells, significant transfection efficiencies with TRD vectors were observed *(figure11-A)*. Expression levels were observed to be substantially higher when cells were transfected with TRDL vectors obtained by addition of Lipofectamine to TRD mixtures *(figure11-B)*.

In primary pulmonary artery cells, such as adventitial fibroblasts (FB$_{PA}$) *(figure11-C)* and smooth muscle cells (SMC$_{PA}$) *(figure11-D)*, TR alone was not sufficient for DNA transfection. However, TRDL vectors significantly improved the luciferase expression levels over that of Lipofectamine standards.

Careful observation of the cells before adding lysis buffer revealed lowered cell viability at higher concentrations of TR. This may be attributed to the decline in transfection efficiency at higher concentrations of TR in A549 cell-line (25µg) as well as FB$_{PA}$ and SMC$_{PA}$ primary cells (4µg).

A

B

C

D
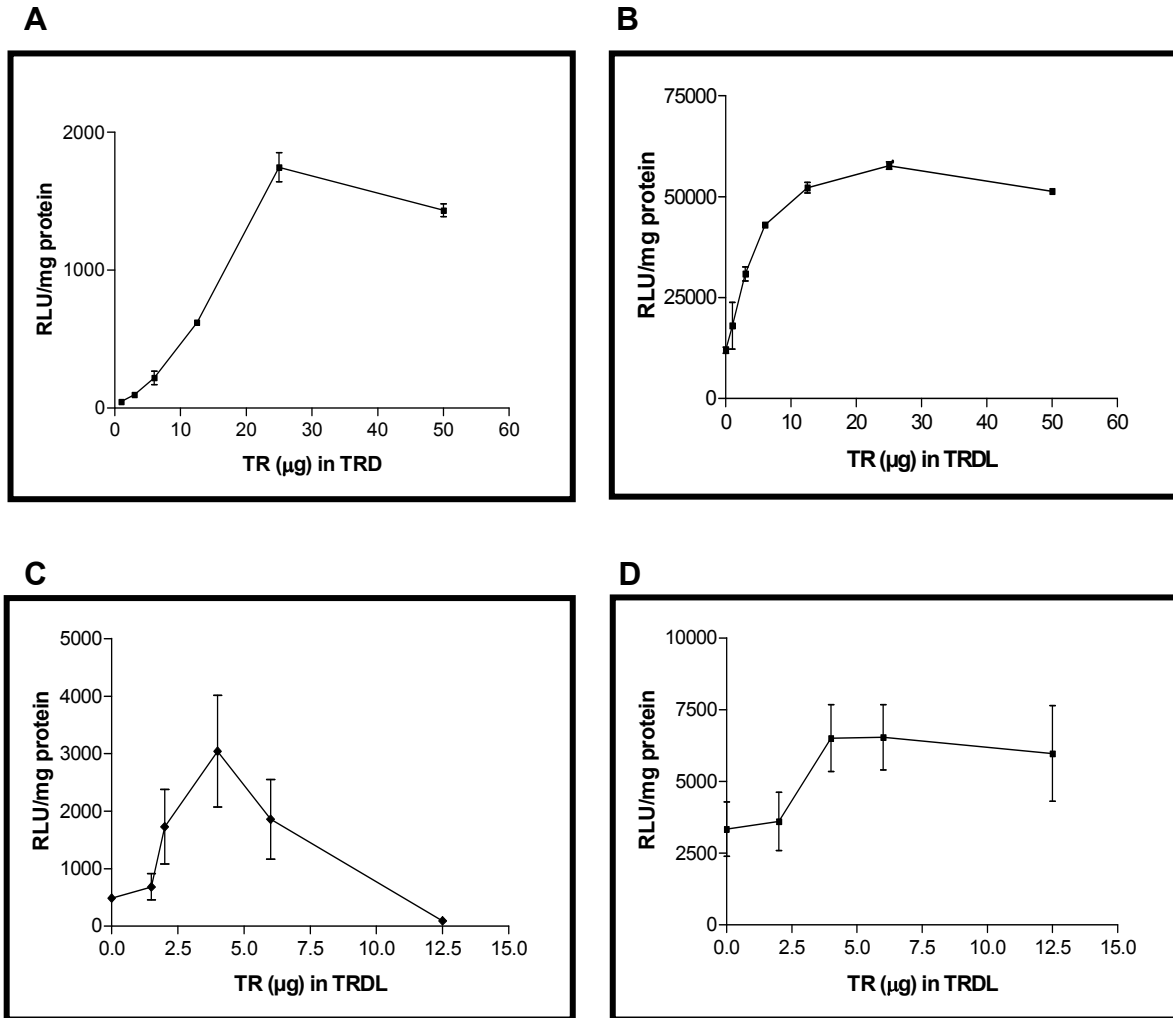
Figure 11: **Dose response in A549, FB$_{PA}$ and SMC$_{PA}$ cells.** Dose response in A549 cells towards TRD (A) and TRDL (B) mediated transfections. Dose response in FB$_{PA}$ (C) and SMC$_{PA}$ (D) primary cells towards TRDL mediated transfections.

3.1.4 Cyto-toxicity assay:

To derive an optimal TR concentration for transfection with minimally compromising cell viability, the cytotoxicitiy associated with different concentrations of TRD and TRDL vectors on the A549 cell-line *(figure12-A)* and FB$_{PA}$ primary cells *(figure12-B)* was assessed. Increasing amounts of TR enhanced the toxicity. Also, the toxicity was enhanced by the addition of Lipofectamine by at least 5% when delivering TRDL into the cells. Further more, the cellular response to test compounds followed the order: TRDL > DL > TRD > D.
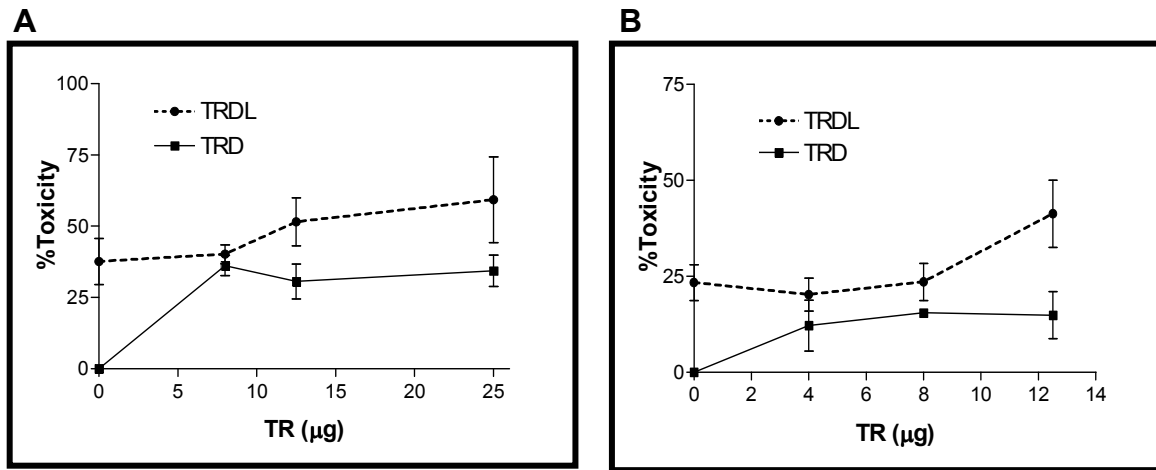
Figure 12: **Cyto-toxicity assay.** Measurement of cytotoxicity in A549 cells (A) and FB_{PA} cells (B) treated by different concentrations of TR in the presence of a given amount (1µg) of DNA (TRD) or of DNA and Lipofectamin (TRDL).

3.1.5 Improvement in transfection efficiency with TRDL vector systems:

Considering the curves of Figures 11 and 12 the optimal concentrations of TR (per microgram of DNA) to be employed in all further analysis using TRDL vectors was estimated as 12.5µg for A549 and 4 µg for FB_{PA} and SMC_{PA}.

The analysis of DNA transfection by TRD, LD, and TRDL was shown in comparison, by measuring the reporter gene luciferase expression in cellular lysate and by counting the GFP positive cells by fluorescence microscopy *(figure13)*.

In A549 cells the transfection efficiencies of TRDL complexes showed 5-fold improvement over the standard lipofectamine (DL) aided transfection. Further, the addition of lipofectamine improved the transfection efficiency of TRD complexes by approximately 30-fold.

In FB_{PA} and SMC_{PA} cells the transfection efficiencies of TRDL vectors showed 3 and 2-fold improvement respectively, over that of DL.

***Figure 13:* TRDL improved transfection efficiency.** Summary on transgene expression levels employing different mixtures of TRD, DL and TRDL as measured by luciferase reporter gene expression in case of pgl3CMV transfection (RLU: relative light units) (left) or by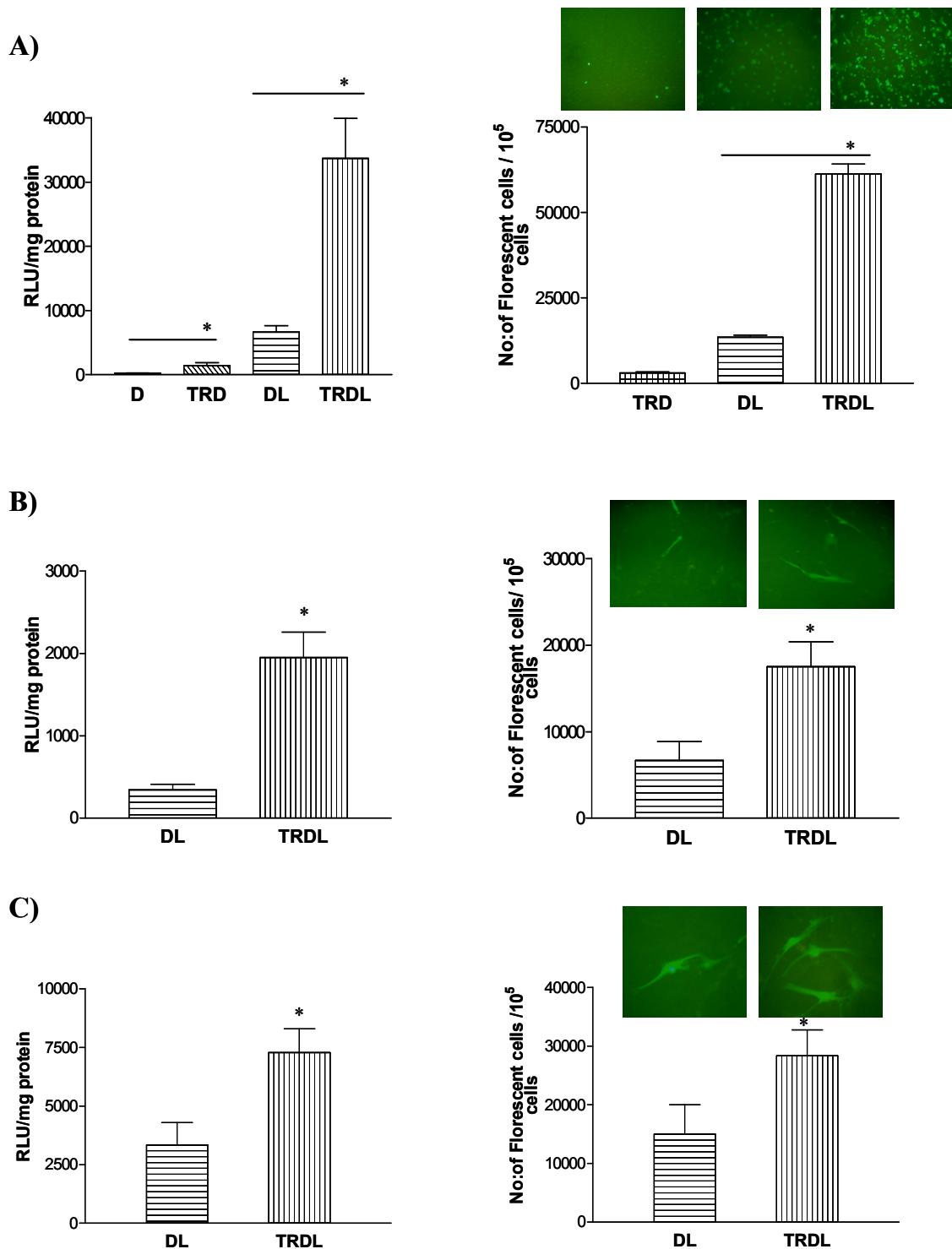 counting number of fluorescent stained cells in case of pEGFP-N2 (right) transfection in A549 (A), FB_{PA} (B) and SMC_{PA} (C) cells.

3.1.6 Analysis of DNA uptake:

For characterization of the facilitated gene transfer, the cellular uptake of fluorescent *Fam* labeled DNA fragments was studied in A549 and FB_{PA} cells transfected with either DL or TRDL. A 409bp fluorescent DNA fragment (*Fam*-CMV) amplified from pgl3CMV *(figure 14-A)* was employed for this purpose. The quantity and integrity of the 409bp fragment was analyzed by capillary gel electrophoresis (Gene Scan) *(figure 14-B)*. Recovering the DNA fragment from the cellular and nuclear compartments of the cells transfected with TRDL and DL vectors exhibited that, TRDL significantly enhanced cellular DNA uptake over that of DL vector system and that the effect is more pronounced in A549 cells *(figure 14-C)* than in FB *(figure 14-D)*.
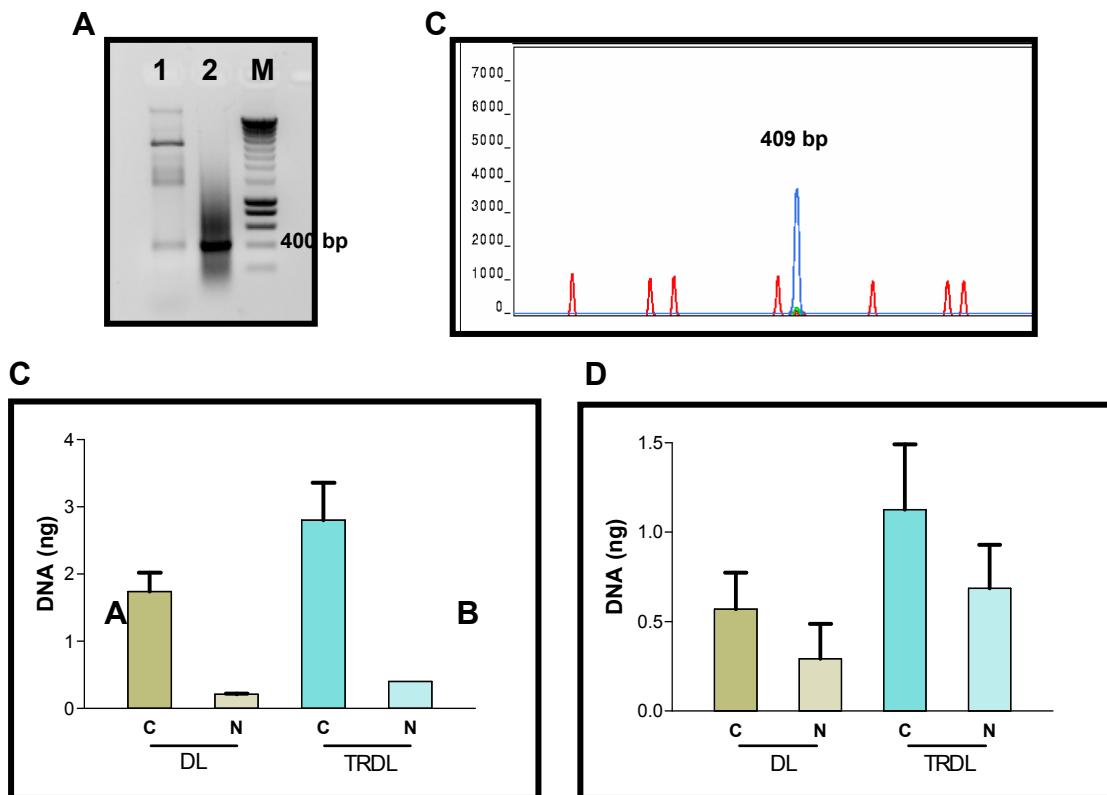
Figure 14: **Analysis of DNA uptake.** *Fam*-CMV is a 409bp fluorescent DNA fragment amplified from pgl3CMV (A) [Lane 1: PCR amplified product from plasmid. The 409bp fragment was excised and gel eluted. Lane 2: PCR product after gel elution. M: Marker]. The quality and integrity of the DNA fragment can be observed from the electropherogram (B). Analysis of DNA uptake revealed higher localization of the fluorescent DNA fragment in the cellular and nuclear compartments with TRDL mediated transfection over that of DL mediated transfection, in both A549 cell-line (C) and FB_{PA} primary cells (D). [C: cellular and N: nuclear compartments]

3.1.7 TRDL transfection efficiency over commercial standards:

Comparison of TRDL mediated transfection with commercially available magnetic beads (CombiMag, Chemicell), Cationic polymer (25 kDa PEI, Aldrich) and cationic lipid (Lipofectamine 2000, Invitrogen) revealed approximately 3.5, 90, 5-fold improvement over CombiMAG, PEI and Lipofectamine 2000 respectively in A549 cells *(figure 15-A)*, 1.3, 23, 3-fold respectively in FB_{PA} cells *(figure 15-B)* and 4, 65, 2-fold respectively in SMC_{PA} cells *(figure 15-C)*.

Figure 15: **TRDL transfection efficiency over commercial standards.** TRDL mediated transfection was observed to be superior over other commercially available transfection agents in A549 cell-line (A) and FB_{PA} (B), SMC_{PA} (C) primary cells.

3.1.8 Immunostaining and confocal imaging:

Caveoli mediated internalization of TRDL complexes:

To explore if the mode of internalization exploited by TRDL vector system is linked with caveoli-mediated endocytosis we performed laser scanning fluorescent confocal microscopic analysis by immune-s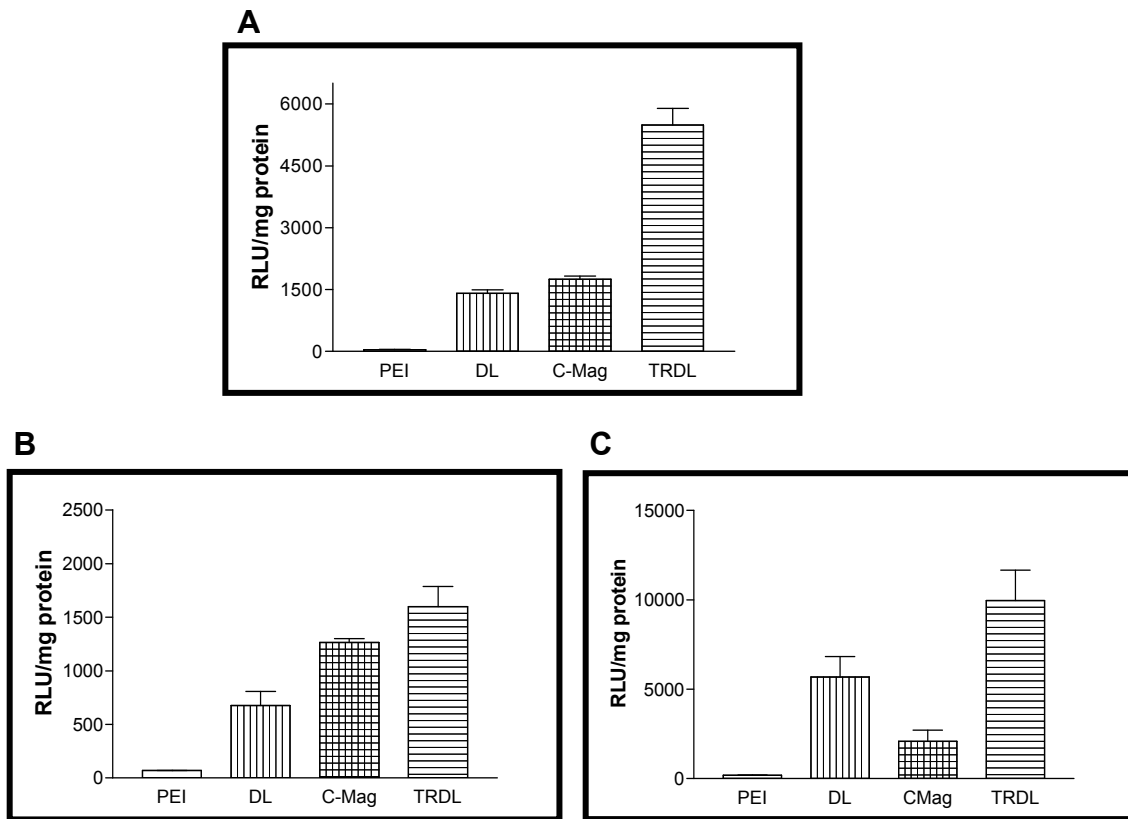taining the cells for caveolin-1 (blue) and TR (red). The cells were not permeabilized to detect only the TR localized at the membrane. In our experiments we found a significant co-localization between caveolin and TR (pink colour). The fluorescent signal of TR was visualized at different time points during transfection (*Figure 16-A: a to c*). The signal was initially localized on the cell membrane. However, a time dependant clearance of the signal from the cell membrane was observed.

In order to show the time dependent cellular internalization of TR, the cells were permeabilized and then stained with streptavidin-Cy3 (red) for intracellular tracking of TR. We observed a strong Cy3 signal at the cell periphery at 2 h, which gradually moved into the cell cytoplasm after longer incubations resulting in a strong cytoplasmic signal after 15 h (*Figure 16-A: d to f*).

In order to examine if DNA internalization corresponded with that of TR, the cells were transfected with a 400 bp *Fam*-labeled DNA fragment using TR and the transfection process was examined by visualizing the uptake of *Fam*-labeled DNA into the cells at different time points (*Figure 16-B: a to c*). We employed Cy3-tagged secondary antibody for caveolin-1 in these experiments and labeled the cytoplasmic and nuclear compartments of the cell with WGA-633 and TO-PRO-3 for the membrane and nucleus, respectively. We observed a strong correlation in time between the cellular internalization of DNA and that of TR.
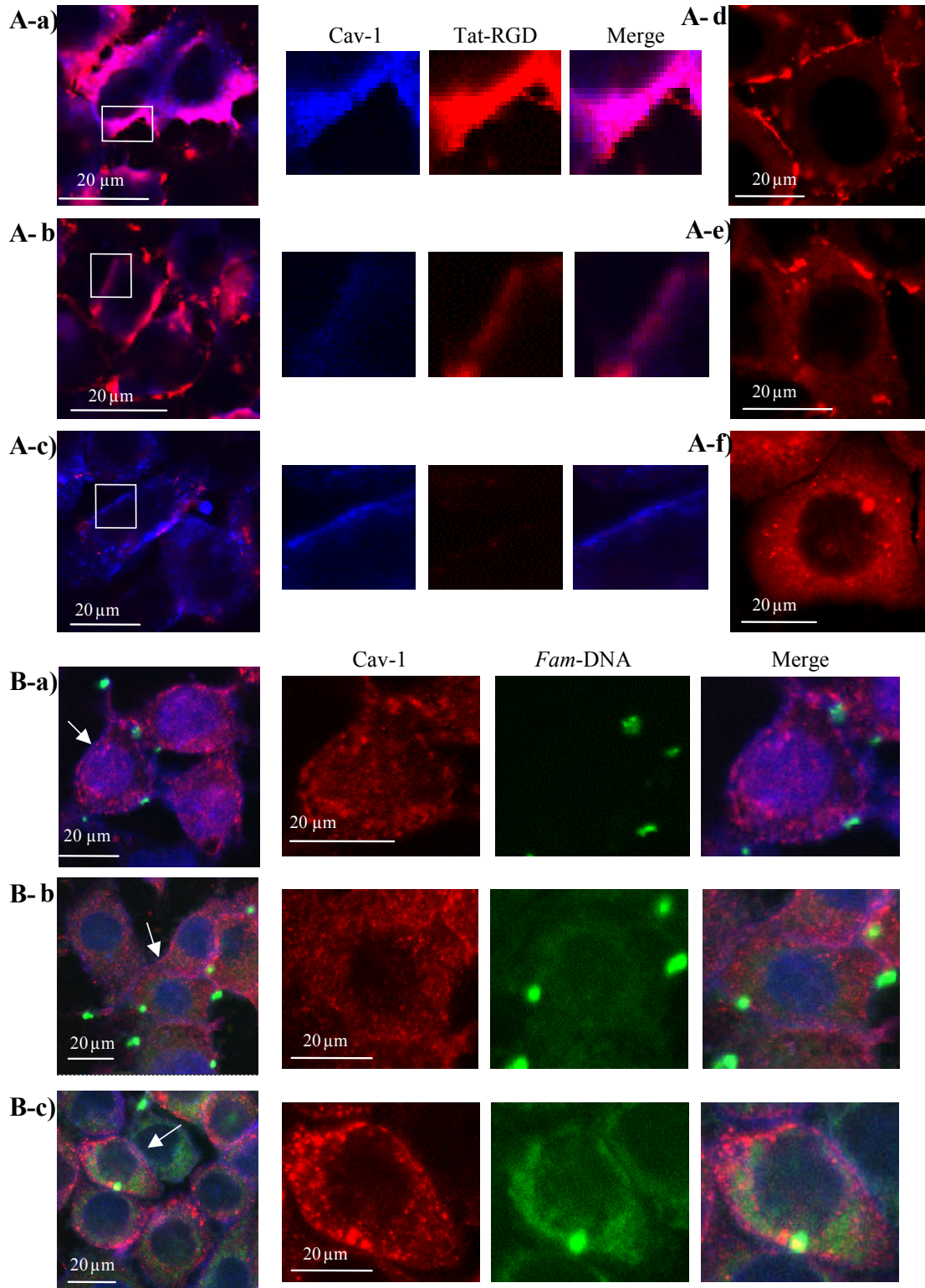
Figure 16: **TatRGD co-localization with Cav-1 and its cellular internalization (A).** A549 cells were transfected with 400bp DNA fragment using TRDL vectors, fixed at 2 h (A-a), 4 h (A-b) and 15 h (A-c) time points and immuno-stained with anti-Cav-1-Cy-5 (blue) and streptavidin-

Cy-3 (red) for caveolins and biotin-TR respectively. We observed co-localization (merge) of TR with Cav-1 (pink) and a time dependant clearance of TR from the cell membrane. When cells were permeabilized and stained with streptavidin-Cy-3, we observed a time dependant internalization of TR (red) into the cytoplasmic compartment of the cells (A-d to f). **TatRGD mediated DNA internalization in cellular compartments (B).** A549 cells were transfected with 400bp *Fam* labeled DNA fragment using TRDL vectors, fixed at 2 h (B-a), 4 h (B-b) and 15 h (B-c) time points and immuno-stained with anti-Cav-1-Cy-3 (red) for Caveolins. In order to distinguish the cellular compartments, the cells were stained with WGA-633 (blue) and TO-PRO-3 (blue) for cell membrane and nucleus respectively. We observed a time dependant cellular internalization of *Fam* labeled DNA, which corresponded with the internalization patterns of TR in permeabilized cells.

 Cellular internalization of TRDL in relation with caveolin expression:

Pulmonary cell-line (A549) and primary cells (SMC$_{PA}$) were transfected with *Fam* labeled DNA fragment and the cells were immuno-stained for Cav-1 (with secondary antibody conjugated with Cy-3). We observed a strong correlation between the DNA (*Fam*) internalization and the expression pattern of caveolins in these cell types. A549 cell-line exhibited strong membrane caveolin staining and also higher *Fam* internalization *(figure 17-A)*. While SMC$_{PA}$ primary cells exhibited weak membrane caveolin staining and also lower *Fam* internalization *(figure 17-B)*

A549 cell-line

SMC$_{PA}$ primary cells
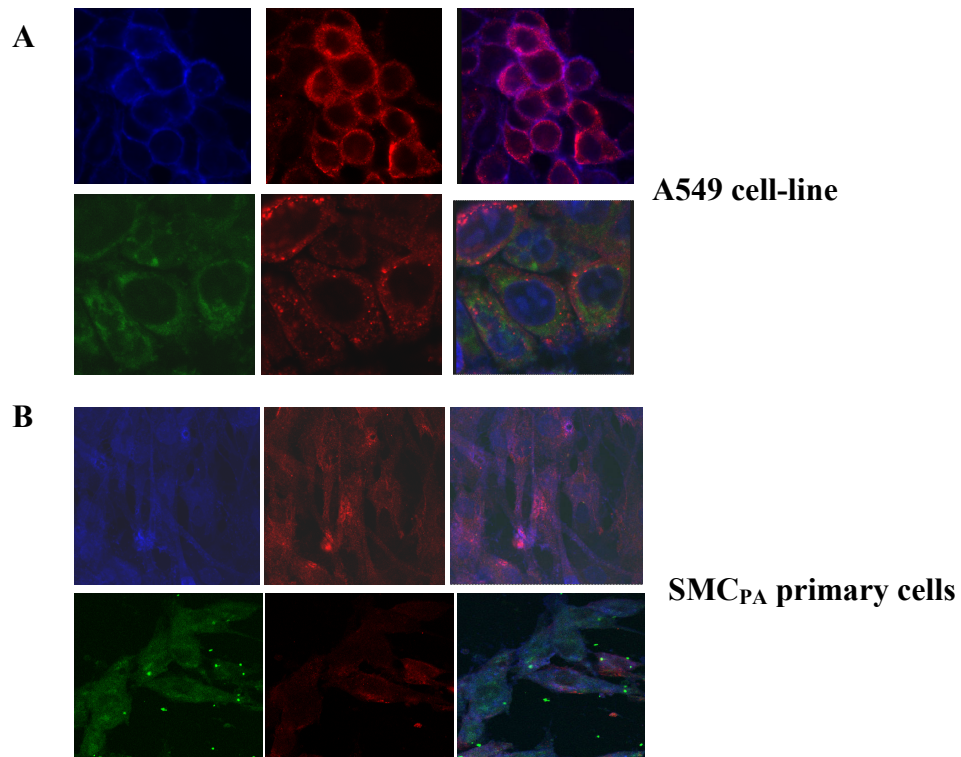
Figure 17: **Cellular internalization of TRDL in relation with caveolin expression**.
A549 cell-line SMC$_{PA}$ primary cells were transfected with *Fam*-DNA (green) employing TRDL
vectors and stained with WGA-633 (blue), TO-PRO-3 (blue), anti-Cav-1-Cy-3 (red) for cell-
membrane, nucleus and caveolins respectively. We observed that, the caveolin staining at the cell
membrane was strong in A549 cells (A: above) and relatively weak in SMC$_{PA}$ cells (B: above).
We observed that, *Fam*-DNA localization in the cellular and nuclear compartments was strong in
A549 cells (A: below) and relatively weak in SMC$_{PA}$ cells (B: below).

3.1.9 Functional assay:

Prevention of Caveoli formation by cholesterol depletion:

To demonstrate further that internalization of TRDL complexes exploit caveolar
endocytic system, we tested the effect of drugs on TRDL mediated internalization.
Methyl-β-cyclodextrin specifically disrupts the formation of caveoli with out interfering
with other modes of endocytosis (**75**). Cells were pretreated with 1% methyl-β-
cyclodextrin for 30 m and transfected with TRDL complexes. Prevention of caveoli
formation drastically decreased the transfection efficiency with TRDL vector system
while that with the standard vector system however remained unaffected *(figure 18),*
suggesting the role of caveoli in the cellular internalization of TRDL complexes.
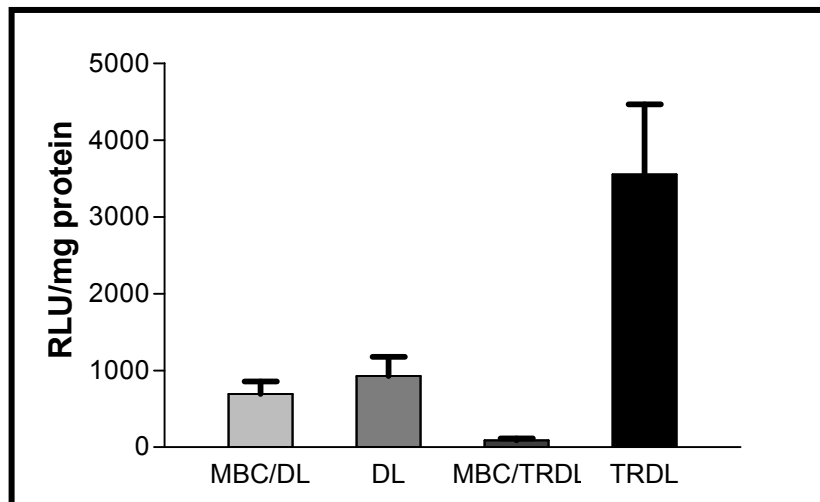
Figure 18: Prevention of Caveoli formation by cholesterol depletion. A549 Cells were pre-
treated with 1% MBC for 30 m and transfected with TRDL and DL vector systems and the
luciferase reporter gene expression was measured. Cells untreated with MBC were taken as
controls for both TRDL and DL transfections.

3.2 Application:

3.2.1 Homology alignment on human RELMβ and mouse HIMF:

We initially isolated a full-length cDNA of RELMβ from human lung tissue RNA by RT-PCR strategy. The nucleic acid sequence (Submitted to EMBL, Acc. No: AM050721) differed at positions 59 and 97 after start of translation from a published sequence (Acc.No. AF323084), resulting in two amino-acid exchanges (proline to leucine and lysine to glutamine). The alignments and homologies of human RELMβ with mouse HIMF on cDNA *(Figure 19-A)* and amino acid *(Figure 19-B)* sequence levels are shown below. Sequence analysis exhibited 69.9% similarity in nucleic acid sequence and 50.4% similarity in amino acid sequence between the human RELMβ and mouse HIMF.

A

```
  1 ggatggggccgtcctcttgcctccttctcatcctaatcccccttctccag  50
    |||||  |  |   |   ||||    |||||||||||    |||  ||||  ||||||
 41 GGATGAAGACTACAACTTGTTCCCTTCTCATCTGCATCTCCCTGCTCCAG  90

 51 ctgatcaacctggggagtactcagtgttccttagactccgttatggatga 100
    |||||   ||   | || ||||| |     || |||  |     |  ||||| |
 91 CTGATGGTCCCAGTGAATACTGATGAGACCATAGAGATTATCGTGGAGAA 140

101 gaagatcaaggatgttctcaacagtctagagtacagtccctctcctataa 150
     |||  |||||||   ||||    || || ||    ||  ||||||  ||  |||
141 TAAGGTCAAGGAACTTCTTGCCAATCCAGCTAACTATCCCTCCACTGTAA 190

151 gcaagaagctctcgtgtgctagtgtcaaaagccaaggcagaccgtcctcc 200
     ||||  |||||  ||  ||||||||||| |       ||||  |  ||||||
191 CGAAGACTCTCTCTTGCACTAGTGTCAAGACTATGAACAGATGGGCCTCC 240

201 tgccctgctgggatggctgtcactggctgtgcttgtggctatggctgtgg 250
    |||||||||||||||||  |||   |||||  |||||||||||||||  ||  ||||||
241 TGCCCTGCTGGGATGACTGCTACTGGGTGTGCTTGTGGCTTTGCCTGTGG 290

251 ttcgtgggatgttcagctggaaaccacctgccactgccagtgcagtgtgg 300
     || ||||||  |  |||   | |   ||  |||  ||||||  ||||    |  |
291 ATCTTGGGAGATCCAGAGTGGAGATACTTGCAACTGCCTGTGCTTACTCG 340

301 tggactggaccactgcccgctgctgccacctgacctgacagg 342
    |  ||||||||||||||||||||||||||||||||||||  |||  |||  |  |
341 TTGACTGGACCACTGCCCGCTGCTGCCAACTGTCCTAAGAAT 382
```

B

```
                .         .          .          .          .
  1 MGPSSCLLLILIPLLQLINLGSTQCSLDSVMDEKIKDVLNSLEYSPSPIS 50
    |  ..| ||| | ||||.   .|   .:: :.: |:|:.| .     || :.
  1 MKTTTCSLLICISLLQLMVPVNTDETIEIIVENKVKELLANPANYPSTVT 50

                .         .          .          .          .
 51 KKLSCASVKSQGRPSSCPAGMAVTGCACGYGCGSWDVQLETTCHCQCSVV 100
    |  ||| |||.    |   .||||||   ||||||: ||||::|    ||.| | .|
 51 KTLSCTSVKTMNRWASCPAGMTATGCACGFACGSWEIQSGDTCNCLCLLV 100

             .
101 DWTTARCCHLT 111
    ||||||||| |.
101 DWTTARCCQLS 111
```

Figure 19: **Sequence alignment of human RELMβ and mouse HIMF:** Alignments of nucleic acid cDNA sequence (top) and amino acid sequence (bottom) of human RELMβ (submitted to EMBL, Acc.No. AM050721) and mouse HIMF (NCBI Acc. No. BC029248) employing GAP software (HUSAR Bioninformatic package). The nucleic acid sequence identity is 69 %. Comparison of the amino acid sequences yields a sequence similarity of 58.6 % and a sequence identity of 49.6 %.

3.2.2 Regulation of RELMβ:

To investigate the expression of RELMβ in different human tissues, human total RNA (Premium RNA, Clontech, BD Biosciences, CA, USA) was employed for semi-quantitative RT-PCR. HIMF specific and HPRT (house keeping) primers were employed for this purpose. Tissue screening of RELMβ expression revealed expression in lung (Lu), heart (H), kidney (K) and adrenal gland (A), whereas in brain (B) and liver (L) no signal was detectable. Highest expression was observed in intestine (C) *(Figure 20-A)*.

Expression analysis of RELMβ in different pulmonary cells was performed employing A549, SMC_{PA} and FB_{PA} cells. RT-PCR analysis was performed using RNA extracts from these cells incubated in normoxic and hypoxic conditions. The RT-PCR results confirmed that the mRNA expression of RELMβ was up-regulated during hypoxia. RELMβ was detected only in +RT and not –RT samples. The expression profiles were controlled by the RT-PCR analysis of a housekeeping gene HPRT *(Figure 20-B)*.

The real-time RT-PCR analysis for RELMβ mRNA expression was performed using RNA extracts from A549, SMC_{PA} and FB_{PA} cells cultured in normoxic (atmospheric) and hypoxic (1% O_2) condition for 24hr (The medium was pre-equilibrated with the respective gas mixture). RELMβ specific and HPRT (housekeeping) primers were

employed for this purpose. The quantitative RT-PCR results confirmed that, expression of RELMβ is up-regulated in hypoxic condition in these cell types. Pronounced hypoxia induced up-regulation of RELMβ expression was observed in A549-epithelial cells and SMC$_{PA.}$ While no specific hypoxia mediated induction of RELMβ was observed in FB$_{PA}$ cells *(Figure 20-C)*.
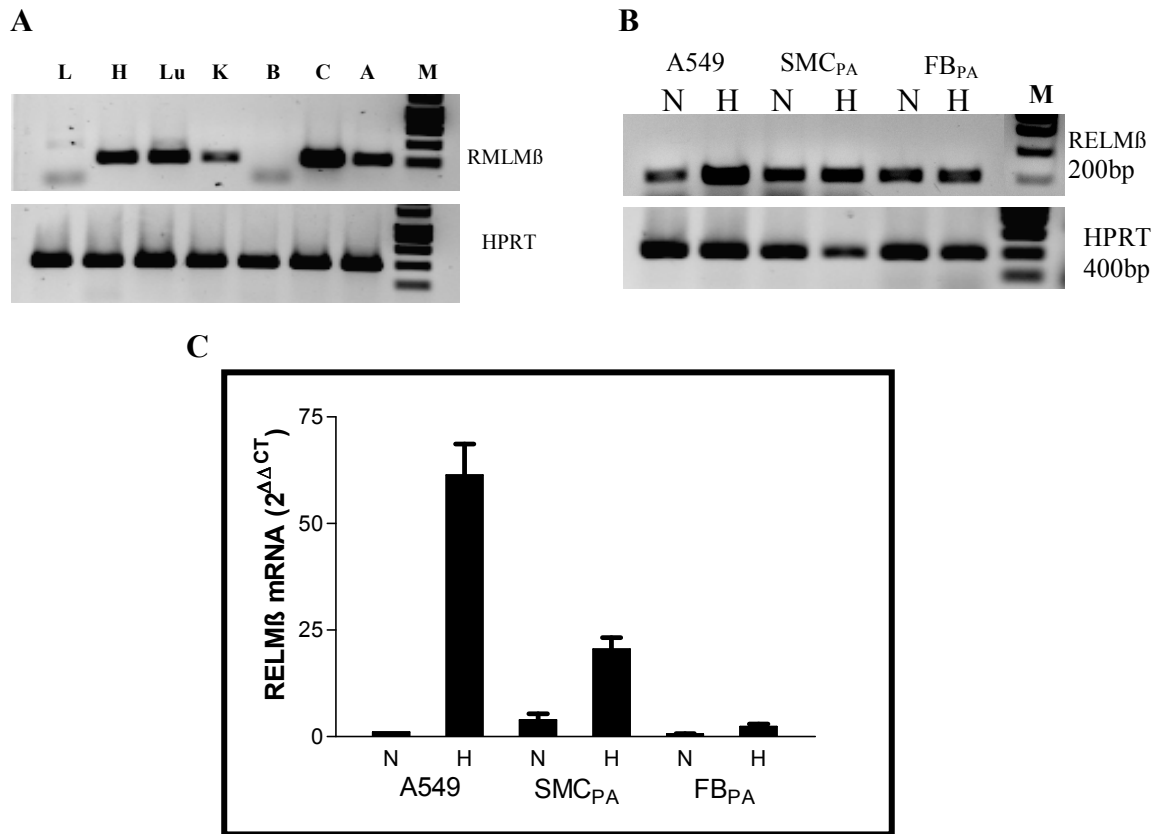

Figure 20: **RELMβ mRNA expression by semi quantitative and quantitative RT-PCR:** Total RNA for human tissues obtained from Clontech was used to analyse the tissue distribution of RELMβ using RT-PCR (A). Total RNA from A549 epithelial cells, SMC$_{PA}$ and FB$_{PA}$ primary cells subjected to normoxic and hypoxic conditions were obtained to analyse the hypoxia induction of RELMβ using RT-PCR analysis (B) and real-time RT-PCR analysis(C). HPRT signals were used as internal controls. Results are shown as the threshold cycle (CT) at which an increase of reporter fluorescence (ΔRn) can first be detected. Amounts of RELMβ mRNA were normalized to HPRT signals and expressed as 2-ΔΔCT. Means ± SE of triplicate samples are shown.

3.2.3 Cloining full length RELMβ:

The full-length RELMβ was cloned into the pGEM-T easy plasmid. Sub-cloning of RELMβ fragment from pGEM-T easy vectors into pCMV-HA vector was performed as mentioned in the methods section.

3.2.4 RELMβ western blot:

Western blot analysis of RELMβ with an HA tag was performed using monoclonal mouse antibody against HA (Sigma Aldrich). Cells were transfected with pCMV-RELMβ-HA and pCMV-HA vectors using DL and TRDL vectors. Protein preparation from the cell lysate was subjected to western blot analysis. The western blot analysis of the cell lysate showed that the expression of HA-tagged RELMβ was higher in cells transfected with TRDL *(Figure 21)* over that of DL. Protein isolated from cells transfected with pCMV-HA was taken as controls. The corresponding β-actin controls were also performed. Thus, transfection and expression of HA-tagged RELMβ was controlled by HA Western-blot analysis
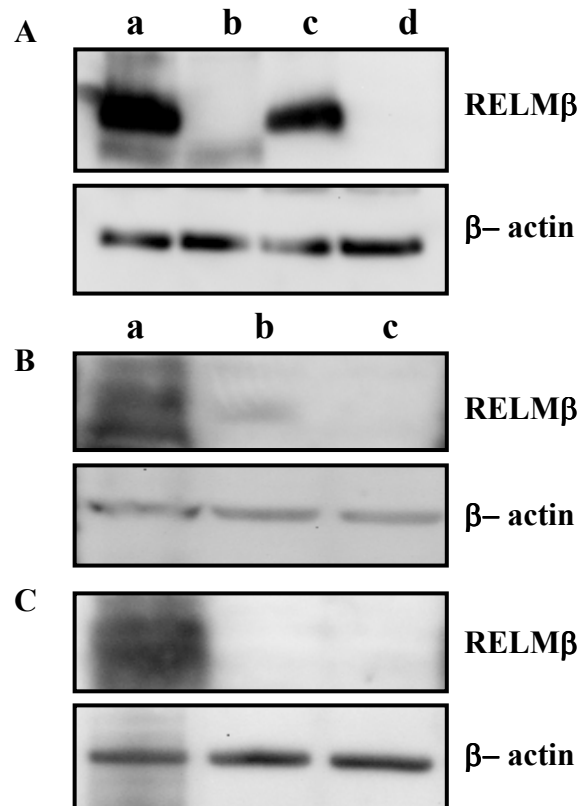
Figure 21: **RELMβ western blot.** Cells over-expressed with RELMβ and cellular extracts were analyzed by HA-Western-blot showing signals only in case of RELMβ-HA-plasmid transfected cells. [A) A549 cells transfected with RELMβ- TRDL (a), control-TRDL (b), RELMβ-DL (c) and control-DL (d). B) SMC$_{PA}$ and C) FB$_{PA}$ cells transfected with RELMβ- TRDL (a), RELMβ-DL (b) and control-DL (c)]

3.2.5 Cell proliferation assay:

Transfected cells were studied with regard to proliferation by measuring the overall cellular mitochondrial respiratory chain activity with MTT assay. Transfection of RELMβ containg vectors and the corresponding control vector was performed using TRDL vectors. Induction of proliferation by RELMβ observed in all investigated cell types was stronger in A549 and SMC$_{PA}$ than FB$_{PA}$ cells *(Figure 22)*. Thus, RELMβ appears to be a hypoxic induced mitogenic factor in human lung cells.
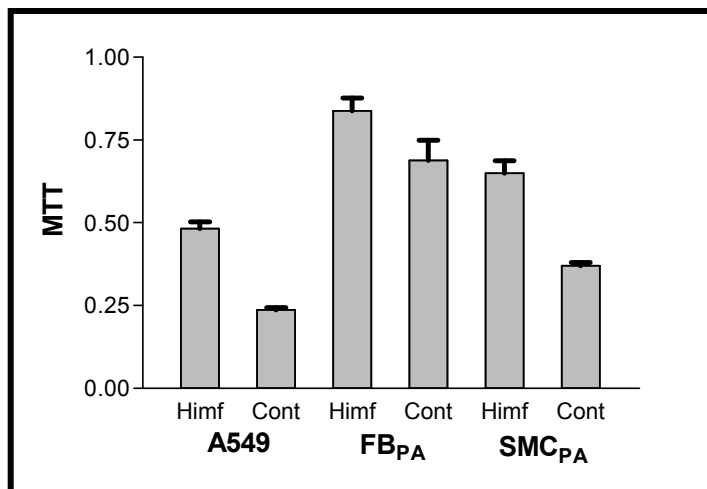

Figure 22: **Cell proliferation.** A549, SMC$_{PA}$ and FB$_{PA}$ cells over expressed with RELMβ and control vectors were subjected to MTT cell proliferation assay. Means ± SE of n=4 samples are shown.

4. Discussion:

4.1 TatRGD mediated gene transfer

In this study, we have analyzed the potency and mode of transfection of pulmonary cells employing the peptide-conjugate TatRGD (TR). HIV-1 derived Tat protein has been described to promote the delivery of proteins or nucleic acids (**57, 58, 60**, **84**). Here, we utilized a truncated 21-mer Tat peptide corresponding to the region between aminoacid residues 43 and 60 consisting of a critical basic aminoacid-stretch (RKKRRQRRR) with 6 arginines. This domain is supposed to be involved in membrane translocation and in nuclear targeting. Particularly, it forms an amphipathic α-helical structure which is involved in endocytosis (**61**). This Tat-peptide was conjugated with a peptide sequence displaying an RGD motif. Particularly, this RGD peptide motif has high affinity towards integrin receptors (αVβ3, α5β1) expressed on cell surfaces and therefore may improve DNA binding to cells. Previous studies have proposed the role of integrin-targeting as an efficient pathway for the uptake of synthetic gene delivery vehicles (**67**). Also, this motif has been described to mediate adenovirus uptake (**66**).

Since this peptide was labeled with biotin we could perform binding studies between DNA and TR. Binding experiments demonstrated affinity between TR and DNA (TRD) which is most likely based on interaction between positively charged Arg of Tat and DNA phosphate backbone. Also, by these experiments a relevant concentration ratio of DNA and TatRGD could be determined.

Particle size measurements revealed lowering of the size of the TRD complexes upon Lipofectamine addition, which is an important feature for successful internalization of these complexes. Further, since the utility of such complexes are largely circumscribed by their high toxicity, we performed cyto-toxicity assays to derive the optimal concentrations of TR for gene transfer in pulmonary cells.

TR was successfully applied for the improvement of DNA delivery into human pulmonary cell-lines and primary cells. Addition of a complex of TR and DNA already yielded in significant transgene expression levels in A549 cells. However, when combining TR with Lipofectamine, the expression was increased 5-fold over Lipofectamine alone (DL) and ~30-fold higher than TRD alone. Therefore, TRD complexes were significantly less efficient than DL and TRDL complexes, indicating the

likely importance of the lipid component in mediating endosomal escape. This observation is consistent with the previous findings on the enhancement of integrin-mediated transfection of haematopoietic cells with synthetic vector systems (**67**).

Similar effect was also observed in primary SMC_{PA} and FB_{PA} cells from pulmonary artery, where transfection efficiencies were enhanced by an approximate factor of 2 and 3-fold, respectively over the DL vector system.

Tracking of fluorescent labelled DNA by capillary electrophoresis confirmed the efficiency of TRDL vectors over DL in A549 and FB_{PA} cells. Further more, the transfected luciferase levels were higher with TRDL vector system by 90, 5 and 3.5 folds in A549 cell-line, 23, 3 and 1.3 folds in FB_{PA} and 65, 2 and 4 folds in SMC_{PA} primary cells, over PEI, DL and CombiMag vector systems respectively.

Biotinylation of TR also allowed the monitoring of its cellular uptake. One possible mechanism to enter cells is mediated by caveoli dependent endocytosis. This pathway has been described for several non-enveloped viruses, some bacterial toxins, membrane constituents and ligands (**78**). Caveoli are invaginated plasma membrane domains characterized by the presence of the integral membrane protein caveolin-1. They are also involved in many endogenous cellular processes like cholesterol homeostasis, glycosphingolipid transport and glycosyl-phosphatidyl-inositol anchored protein recycling (**79**). There is also evidence that HIV-1 Tat (**67**) and HIV-1 virus itself (**85**) can use caveoli for transcytosis across the endothelium. We investigated if TR-D-L internalization follows caveoli-mediated pathway. Our confocal microscopic analysis revealed co-localization of TatRGD and Caveolin-1 in A549 cells transfected with TRDL vector systems. We also observed a time dependent clearance of TR from the cell membrane. The cells were permeabilized to observe the cellular internalization of TR. At 2 h incubation the TR signal was confined to the cell membrane, after 4 h we observed moderate amounts of signal in the cytoplasm and after 15 h incubation we observed the maximum signal in the cytoplasm. Corresponding time dependant internalization of *F*AM labeled DNA was also observed. Therefore TR containing vector are internalized through a slow internalization process similar to that observed with full length Tat internalization (**67**). This slow movement is incompatible with the fast dynamics described for constitutive endocytic trafficking of clathrin-coated pits and vesicles (**79**). Slow dynamics

associated with endocytic pathway was recently demonstrated to involve a non-constitutive and highly stable Caveolin-1 positive endocytic pathway in transfected HeLa cells (**81**).Additional evidences for this mechanism and its dynamics can be found elsewhere (**82**).

To further demonstrate that TRDL complexes undergo caveoli-mediated internalization, caveoli disruption was performed employing the inhibitor methyl-β-cyclodextrin This drug has been described to affect caveoli mediated but not clathrin-mediated endocytosis (**75, 83**). Treatment of cells with methyl-β-cyclodextrin drastically decreased the transfection efficiency of TatRGD. Interestingly, primary SMC_{PA} that showed less TR dependent transfection efficiency also revealed reduced levels of calveolin-1 expression when compared to A549 cells in immune-cytochemical analysis. Therefore we suggest a strong correlation between TR mediated DNA internalization and the expression pattern of caveolins in these cell types.

In conclusion, the present work indicates that the TatRGD peptide mediates efficient gene delivery in human pulmonary cells. In particular, the combination of TatRGD with standard cationic lipid based transfection reagent resulted in enhanced gene transfer. The improved DNA uptake by TatRGD appears to be mediated by caveoli dependent endocytosis. Thus, TatRGD can to be considered as a peptide that favours DNA uptake in lung cells and may also be considered as a transfection option for other transfection resistant cell types.

4.2 Human RELM-β is a mitogenic factor in lung cells and induced in hypoxia

In this study we have analyzed the gene expression, hypoxic regulation and proliferative effects of RELMβ in human lung cells. Our study was inspired by investigations on the related HIMF gene in mouse also described in other context as RELMα, or FIZZ1 (**72**). Human RELMβ represents the most homolog gene of mouse HIMF, however is not considered as the human ortholog gene of mouse HIMF, which appears not to exist (**71**). Tissue screening of RELMβ expression revealed expression in lung, heart and kidney, highest expression in intestine, whereas in brain and liver no signal was detectable. Since HIMF plays an important role in hypoxic adaptive processes in lung physiology in mouse, we have analyzed the expression, hypoxic regulation and proliferative responses of RELMβ in human lung cells. We found strong hypoxic induction of RELMβ in lung epithelial A549 cells and primary vascular cells from pulmonary artery. In transfected RELMβ overexpressing cells, significant proliferative effects in the studied cells were observed. Thus, this study suggests that RELMβ in human is similar regulated as described for HIMF in the in vivo mouse experiments and acts as a proliferative factor. Consequently, RELMβ in human may play a role in hypoxic induced pulmonary remodelling leading to pulmonary hypertension. Also, the induction and proliferative responses of RELMβ may play a role in fibrotic lung disease which is associated with hypoxia.

Further findings of HIMF were explored in mice experiments. Beside proliferative effects, HIMF was demonstrated to have angiogenic and vasoconstrictive properties (**72**). Additionally, HIMF also was shown to play a role in lung development, by regulation of apoptosis and participation in alveolarization and lung maturation (**86**) and compensatory lung growth after pneumectomy (**73**). Also, HIMF (FIZZ1) was shown to be strongly increased during allergic pulmonary inflammation (**68**). The exploration of these characteristics regarding RELMβ in human remains open. So far, functional aspects of RELMβ and resistin have been mainly described in mice with respect to resistence to insulin (**70, 87, 88**). Resistin, mainly expressed in adipocytes and RELMβ, expressed particularly expressed in epithelial cells from intestine, were demonstrated to mediate resistance to insulin leading to increased glucose production.

In sum, our study revealed new findings for human RELMβ as a factor which is induced in hypoxia and which exerts proliferative effects. These effects were observed in human primary vascular cells from pulmonary artery and a lung epithelial cell line. Thus human RELMβ resembles features as described for the related HIMF described in the lung of mice.

Perspective:

The present work revealed in it's first part that TatRGD is an appropriate tool for the improvement of transfection of Plasmid-DNA as studied in cultured human lung cells. Future perspectives of transfection by TatRGD may comprise:

1. Application of this technique for theoretical-experimental purpose regarding the functional characterization of further human genes in lung cells.
2. Potential adaptation of TatRGD mediated transfection to 'small' nucleic acids as antisense oligonucleotides or small interfering RNAs (siRNAs) for the inhibition of gene expression.
3. Employment and adaptation of TatRGD technique for DNA-transfection *in vivo* in animal experiments targeting the lungs by airway access or via pulmonary artery. Potential immune responses and toxicity effects are important issues that could be examined in this context.

In the second part, this study revealed important new functional and regulatory findings of human RELMβ gene in pulmonary cells. These findings on RELMβ raise several questions which may be addressed in future studies:

a. Is the regulation of RELMβ in hypoxia directly dependent on hypoxia-inducible-factors (HIF)? Does the regulatory regions of the RELMβ gene contain hypoxia-responsive –elements?
b. What is the mechanism of induction of proliferation by RELMβ: which transduction pathway and which second messengers are involved?
c. Which receptors are responsible for mediating the observed effects of RELMβ?

Summary:

The presented study is organized in two sections. In the first part a DNA-transfection procedure for human lung cells employing a peptide conjugate has been established and the corresponding transfection process characterized. In the second part this new transfection strategy has been applied for studying functional aspects of the human RELM-β gene.

Cell-lines and primary cells exhibit a varying degree of resistance to DNA transfection strategies. In this study, we employed the synthetic peptide TatRGD (TR), composed of the HIV-1 derived translocation peptide *Tat* fused to the integrin binding *RGD* motif, as a tool for improving DNA transfer into human pulmonary cells. Binding experiments between DNA and TR and cytotoxicity measurements of TR treated cells were undertaken to optimize DNA and TR concentrations for transfection. Addition of a complex of TR and DNA (TRD) to A549 cells yielded in significant transgene expression. When combining TRD with Lipofectamine (TRDL), the expression was increased by 5-fold over Lipofectamine (DL) and by ~30-fold over TRD mediated transfections. Also, in primary smooth muscle cells (SMC) and fibroblasts (FB) derived from pulmonary arteries, an increase in TRDL mediated transfection efficiency was observed by a factor of ~ 2 and ~ 3 over that of DL. Laser scanning confocal microscopy for visualizing TR dependent DNA uptake demonstrated that the internalization of TRDL complexes is linked to caveoli in the plasma membrane. Interfering caveoli formation by methyl-b-cyclo-dextrin drastically decreased the transfection efficiency by TR. In conclusion, the TatRGD peptide mediates efficient gene delivery in human pulmonary cells, in particular when combined with standard cationic lipid based transfection reagent. The enhancement of DNA uptake by TatRGD is suggested to be mediated by caveoli dependent endocytosis.

RELMβ (resistin-like molecule) represents the most related human homologue of mouse RELMα also known as hypoxic-induced-mitogenic-factor (HIMF) for which no human orthologue gene exist. In this part of the study, we isolated RELMβ cDNA from human lung tissue and performed regulatory and functional expression studies with the TatRGD

procedure. RELMβ mRNA was upregulated in hypoxia in human lung A549 cell line as well as primary cultured adventitial fibroblasts (FB) and smooth muscle cells (SMC) of pulmonary artery. Upon transfection of a RELMβ encoding expression plasmid into these cells, we observed significant induction of proliferation particularly in SMC and A549 cells. The results suggest that human RELMβ may contribute to hypoxic induced pulmonary vascular remodeling processes or hypoxia related fibrotic lung disease.

Zusammenfassung:

Die vorgelegte Studie ist in zwei Abschnitte gegliedert. Im ersten Teil wird eine DNA-Transfektions Prozedur mit Hilfe eines Peptid-Konjugats etabliert und der zugehörige Transfektions Prozess charakterisiert. Im zweiten Teil wird diese Transfektions Strategie angewendet, um funktionelle Aspekte des humanen RELM-β Gens zu untersuchen.

Zelllinien und primäre Zellen zeigen eine unterschiedliche Resistenz gegenüber DNA-Transfektions Methoden. In dieser Studie wurde das synthetische Peptid TatRGD (TR), das aus dem von HIV-1 abgeleitetem Translokations Peptid *Tat* und dem Integrin bindenden *RGD* Motiv zusammengesetzt ist, genutzt, um den DNA Transfer in humane pulmonale Zellen zu begünstigen. Bindungsexperimente zwischen DNA und TR, sowie Zytotoxizitäts Messungen von TR behandelten Zellen wurden durchgeführt, um die zu verwendenden DNA und TR Konzentrationen zu optimieren. Zugabe eines Komplexes von TR und DNA (TRD) zu A549 Zellen resultierte in signifikanter transgener Expression. Die Kombination von TRD und Lipofectamin (TRDL) verstärkte die Expression 5-fach gegebenüber Lipofectamin (DL) und 30-fach gegenüber TRD vermittelter Transfektion. Ebenso in primär kultivierten glatten Muskelzellen (SMC) und adventitialen Fibroblasten (FB), die aus Pulmonalarterien gewonnen wurden, wurde eine Steigerung der Transfektionseffizienz um den Faktor 2 bzw. 3 gegenüber DL beobachtet. Laser-Scan basierte konfokale Mikroskopie zeigte, dass die TR abhängige DNA Aufnahme abhängig von Caveolae in der Plasmamembran ist. Inhibition der Caveolae Bildung durch Methyl-b-Cyclo-Dextrin verminderte drastisch die Transfektions Effizienz durch TR. Zusammengefasst, vermittelt TatRGD einen effizienten DNA Transfer in humane pulmonale Zellen, insbesondere wenn es mit Transfektions Reagenzien, die auf kationischen Lipiden basieren, kombiniert wird. Die Steigerung der DNA Aufnahme wird vermutlich durch Caveolae-abhängige Endozytose vermittelt.

RELMβ (resistin-like molecule) repräsentiert das am nächsten homologe Gen von RELMα der Maus, das auch unter dem Namen HIMF (hypoxic-induced-mitogenic-factor) bekannt ist, für das aber kein orthologes humanes Gen existiert. In diesem Teil der Studie isolierten wir RELMβ cDNA von humanem Lungen Gewebe und führten

funktionelle Expressions Studien mittels der TatRGD Methode sowie Untersuchungen zu seiner Regulation durch. Wir beobachteten eine Hochregulation von RELMβ mRNA in Hypoxie in der epithelialen humanen Lungenzellinie A549 sowie in primär kultivierten FB und SMC der Pulmonalarterie. Nach Transfektion der Zellen mit einem Expressionsplasmid kodierend für RELMβ beobachteten wir eine signifikante Induktion der Proliferation insbesondere in SMC und A549 Zellen. Die Ergebnisse weisen darauf hin, dass humanes RELMβ am pulmonal-arteriellen Remodeling Prozess in Hypoxie oder an Hypoxie-assoziierten fibrotischen Lungenerkrankungen beteiligt sein könnte.

References:

1. Fannon MR. Gene expression in normal and disease states-identification of therapeutic targets, *Trends Biotechnol,* 1996, **14**(8): 294-8

2. Chang PL, Bowie KM. Development of engineered cells for implantation in gene therapy, *Adv Drug Del Rev,* 1998, **33**: 31-43

3. Anderson WF. Human gene therapy, *Nature* 1998, **392** (6679 Suppl): 25-30

4. Kawabata K, Takakura Y, Hashida M. The fate of plasmid DNA after intravenous injection in mice: involvement of scavenger receptors in its hepatic uptake, *Pharm Res,* 1995, **12**(6): 825-30

5. Ledley FD. Pharmaceutical approach to somatic gene therapy, *Pharm Res,* 1996, **13**(11): 1595-614

6. Plank C, Anton M, Rudolph C, Rosenecker J, Krotz F. Enhancing and targeting nucleic acid delivery by magnetic force, *Expert Opin Biol Ther,* 2003, **3**(5): 745-58

7. Wells DJ. Gene therapy progress and projects: electroporation and other physical methods, *Gene Ther,* 2004, **11**(18): 1363 – 9

8. Kotnik T, Bobanovic F and Miklavcic D. Sensitivity of transmembrane voltage induced by applied electric fields – a theoretical analysis, *Bioelectrochem Bioenerget,* 1997, **43**: 285–291.

9. Kotnik T, Miklavcic D and Slivnik T. Time course of transmembrane voltage induced by time-varying electric fields – a method for theoretical analysis and its application, *Bioelectrochem Bioenerget,* 1998, **45**: 3–16

10. Teissie J and Rols M.P. An experimental evaluation of the critical potential difference inducing cell membrane electropermeabilization, *Biophys J,* 1993, **65**: 409–413.

11. Teissie J and Rols, M.P. Manipulation of cell cytoskeleton affects the lifetime of cell membrane electropermeabilization, *Ann NY Acad Sci,* 1994, **720**: 98–110.

12. Plank C, Scherer F, Schillinger U, Bergemann C, Anton M. Magnetofection: enhancing and targeting gene delivery with superparamagnetic nanoparticles and magnetic fields, *J Liposome Research,* 2003, **13**(1): 29-32.

13. Plank C, Anton M, Rudolph C, Rosenecker J, Krotz F. Enhancing and targeting nucleic acid delivery by magnetic force, *Expert Opin Biol Ther,* 2003, **3**(5): 745-58.

14. Huth S, Lausier J, Gersting SW, Rudolph C, Plank C, Welsch U, Rosenecker J. Insights into the mechanism of magnetofection using PEI-based magnetofectins for gene transfer, *J Gene Med,* 2004, **6**: 923–936.

15. Budker V, Budker T, Zhang G, Subbotin V, Loomis A, Wolff JA. Hypothesis: naked plasmid DNA is taken up by cells in vivo by a receptor-mediated process, *J Gene Med,* 2000, **2**(2):76-88.

16. Felgner PL, Gadek TR, Holm M, Roman R, Chan HW, Wenz M. Lipofection: a highly efficient, lipid-mediated DNA-transfection procedure, *Proc Natl Acad Sci USA,* 1987, **84**(21): 7413-7.

17. Perelson AS, Macken CA, Grimm EA, Roos LS, Bonavida B. Mechanism of cell-mediated cytotoxicity at the single cell level. VIII. Kinetics of lysis of target cells bound by more than one cytotoxic T lymphocyte, *J Immunol,* 1984, **132**(5): 2190-8.

18. Bertrand JR, Pottier M, Vekris A, Opolon P, Maksimenko A, Malvy C. Comparison of antisense oligonucleotides and siRNAs in cell culture and in vivo, *Biochem Biophys Res Commun* 2002, **296**(4): 1000-4.

19. Xia H, Mao Q, Paulson HL, Davidson BL. siRNA-mediated gene silencing in vitro and in vivo, *Nat Biotechnol,* 2002, **20**(10): 1006-10.

20. Ferrari ME, Nguyen CM, Zelphati O, Tsai Y, Felgner PL. Analytical methods for the characterization of cationic lipid-nucleic acid complexes, *Hum Gene Ther,* 1998, **9**(3): 341-51.

21. Felgner JH, Kumar R, Sridhar CN, Wheeler CJ, Tsai YJ, Border R. Enhanced gene delivery and mechanism studies with a novel series of cationic lipid formulations, *J Biol Chem,* 1994, **269**(4): 2550-61.

22. Wang J, Guo X, Xu Y, Barron L, Szoka FC, Jr. Synthesis and characterization of long chain alkyl acyl carnitine esters. Potentially biodegradable cationic lipids for use in gene delivery, *J Med Chem,* 1998, **41**(13): 2207-15.

23. MacDonald RC, Rakhmanova VA, Choi KL, Rosenzweig HS, Lahiri MK. O-ethylphosphatidylcholine: A metabolizable cationic phospholipid which is a serum-compatible DNA transfection agent, *J Pharm Sci,* 1999, **88**(9): 896-904.

24. Byk G, Dubertret C, Escriou V, Frederic M, Jaslin G, Rangara R, et al. Synthesis, activity, and structure--activity relationship studies of novel cationic lipids for DNA transfer, *J Med Chem,* 1998, **41**(2):229-35.

25. Sternberg B, Sorgi FL, Huang L. New structures in complex formation between DNA and cationic liposomes visualized by freeze-fracture electron microscopy, *FEBS Lett,* 1994, **356**(2-3): 361-6.

26. Gershon H, Ghirlando R, Guttman SB, Minsky A. Mode of formation and structural features of DNA-cationic liposome complexes used for transfection, *Biochemistry,* 1993, **32**(28): 7143-51.

27. Radler JO, Koltover I, Salditt T, Safinya CR. Structure of DNA-cationic liposome complexes: DNA intercalation in multilamellar membranes in distinct interhelical packing regimes, *Science,* 1997, **275**(5301): 810-4.

28. Gustafsson J, Arvidson G, Karlsson G, Almgren M. Complexes between cationic liposomes and DNA visualized by cryo-TEM, *Biochim Biophys Acta,* 1995, **1235**(2): 305-12.

29. Lasic DD, Strey H, Stuart MCA, Pogdornik R, Frederik PM. The structure of DNA-liposome complexes, *JACS,* 1997, **119**(4): 832-3.

References

30. Mok KW, Cullis PR. Structural and fusogenic properties of cationic liposomes in the presence of plasmid DNA, *Biophys J,* 1997, **73**(5): 2534-45.

31. Koltover I, Salditt T, Radler JO, Safinya CR. An inverted hexagonal phase of cationic liposome-DNA complexes related to DNA release and delivery, *Science,* 1998, **281**(5373): 78-81.

32. Xu Y, Hui SW, Frederik P, Szoka FC, Jr. Physicochemical characterization and purification of cationic lipoplexes, *Biophys J,* 1999, **77**(1): 341-53.

33. Turek J, Dubertret C, Jaslin G, Antonakis K, Scherman D, Pitard B. Formulations which increase the size of lipoplexes prevent serum-associated inhibition of transfection, *J Gene Med,* 2000, **2**(1): 32-40.

34. Ross PC, Hui SW. Lipoplex size is a major determinant of in vitro lipofection efficiency, *GeneTher,* 1999, **6**(4): 651-9.

35. Kennedy MT, Pozharski EV, Rakhmanova VA, MacDonald RC. Factors governing the assembly of cationic phospholipid-DNA complexes, *Biophys J,* 2000, **78**(3): 1620-33.

36. Mahato RI, Smith LC, Rolland A. Pharmaceutical perspectives of nonviral gene therapy, *Adv Genet,* 1999, **41**: 95-156.

37. Zelphati O, Uyechi LS, Barron LG, Szoka FC, Jr. Effect of serum components on the physico-chemical properties of cationic lipid/oligonucleotide complexes and on their interactions with cells, *Biochim Biophys Acta,* 1998, **1390**(2): 119-33.

38. Hong K, Zheng W, Baker A, Papahadjopoulos D. Stabilization of cationic liposome-plasmid DNA complexes by polyamines and poly(ethylene glycol)-phospholipid conjugates for efficient in vivo gene delivery, *FEBS Lett,* 1997, **400**(2): 233-7.

39. Meyer O, Kirpotin D, Hong K, Sternberg B, Park JW, Woodle MC. Cationic liposomes coated with polyethylene glycol as carriers for oligonucleotides, *J Biol Chem,* 1998, **273**(25): 15621-7.

40. Mok KW, Lam AM, Cullis PR. Stabilized plasmid-lipid particles: factors influencing plasmid entrapment and transfection properties, *Biochim Biophys Acta,* 1999, **1419**(2): 137-50.

41. Wu GY, Wu CH. Receptor-mediated in vitro gene transformation by a soluble DNA carrier system, *J Biol Chem,* 1987, **262**(10): 4429-32.

42. Golan R, Pietrasanta LI, Hsieh W, Hansma HG. DNA toroids: stages in condensation, *Biochemistry,* 1999, **38**(42): 14069-76.

43. Adami RC, Collard WT, Gupta SA, Kwok KY, Bonadio J, Rice KG. Stability of peptide-condensed plasmid DNA formulations, *J Pharm Sci* 1998, **87**(6): 678-83.

44. Duguid JG, Li C, Shi M, Logan MJ, Alila H, Rolland A. A physicochemical approach for predicting the effectiveness of peptide-based gene delivery systems for use in plasmid-based gene therapy, *Biophys J* 1998, **74**(6): 2802-14.

45. Lee H, Jeong JH, Park TG. PEG grafted polylysine with fusogenic peptide for gene delivery: high transfection efficiency with low cytotoxicity, *J Control Release,* 2002, **79**(1-3): 283-91.

46. Mannisto M, Vanderkerken S, Toncheva V, Elomaa M, Ruponen M, Schacht E, et al. Structure-activity relationships of poly (L-lysines): effects of pegylation and molecular shape on physicochemical and biological properties in gene delivery, *J Control Release,* 2002, **83**(1):169-82.

47. Lee RJ, Huang L. Folate-targeted, anionic liposome-entrapped polylysine-condensed DNA for tumor cell-specific gene transfer, *J Biol Chem* 1996, **271**(14): 8481-7.

48. Vitiello L, Chonn A, Wasserman JD, Duff C, Worton RG. Condensation of plasmid DNA with polylysine improves liposome-mediated gene transfer into established and primary muscle cells, *Gene Ther,* 1996, **3**(5): 396-404.

49. Gao X, Huang L. Potentiation of cationic liposome-mediated gene delivery by polycations, *Biochemistry,* 1996, **35**(3): 1027-36.

50. Boussif O, Lezoualc'h F, Zanta MA, Mergny MD, Scherman D, Demeneix B, et al. A versatile vector for gene and oligonucleotide transfer into cells in culture and in vivo: polyethylenimine, *Proc Natl Acad Sci U S A,* 1995, **92**(16): 7297-301.

51. Dick RC, Ham GE. Characterization of polyethylenimine, *J Macromol Sci,* 1997, **A4**:1301-1314.

52. Fischer D, Bieber T, Li Y, Elsasser HP, Kissel T. A novel non-viral vector for DNA delivery based on low molecular weight, branched polyethylenimine: effect of molecular weight on transfection efficiency and cytotoxicity, *Pharm Res,* 1999, **16**(8): 1273-9.

53. Goula D, Remy JS, Erbacher P, Wasowicz M, Levi G, Abdallah B. Size, diffusibility and transfection performance of linear PEI/DNA complexes in the mouse central nervous system, *Gene Ther,* 1998, **5**(5): 712-7.

54. Katayose S, Kataoka K. Water-soluble polyion complex associates of DNA and poly (ethylene glycol)-poly(L-lysine) block copolymer, *Bioconjug Chem,* 1997, **8**(5): 702-7.

55. Ahn CH, Chae SY, Bae YH, Kim SW. Biodegradable poly (ethylenimine) for plasmid DNA delivery, *J Control Release,* 2002, **80**(1-3): 273-82.

56. Choi YH, Liu F, Choi JS, Kim SW, Park JS. Characterization of a targeted gene carrier, lactose-polyethylene glycol-grafted poly-L-lysine and its complex with plasmid DNA, *Hum Gene Ther,* 1999, **10**(16): 2657-65.

57. Fawell S, Serry J, Daikh Y, Moore C, Chen LL, Pepinsky B, Barsoum J. Tat-mediated delivery of heterologous proteins into cells, *Proc Natl Acad Sci USA*, 1994, **91**: 664-668.

58. Schwarze SR, Ho A, Akbani AV, Dowdy SF. In vivo protein transduction: Delivery of a biologically active protein into the mouse, *Science,* 1999, **285**(3): 1569-1572.

59. Futaki S, Suzuki T, Ohashi W, Yagami T, Tanaka S, Ueda K, Sugiura Y. Arginine-rich Peptides: An abundant source of membrane permeable peptides having potential as carriers for intracellular protein delivery, *J Biol Chem,* 2001, **276**(8): 5836-5840.

60. Jeang KT, Xiao H, Rich EA. Multifaceted activities of the HIV-1 transactivator of Transcription-Tat, *J Biol Chem,* 2001, **274**(41): 28837-40.

61. Eric V, Priscille B, Bernard L. A truncated HIV-1 Tat protein basic domain rapidly translocates through the plasma membrane and accumulates in the cell nucleus, *J Biol Chem,* 1997, **272**(25): 16010 – 16017.

62. Akiko E, Teruo A, Hajime O, Takao S, HaruhikoY, Hachiro I, Shigeo F, Takao H, Katsuo T, Mamoru H, Mahito N. Protein transduction domain of HIV-1 Tat protein promotes efficient delivery of DNA into mammalian cells. *J Biol Chem,* 2001, **276** (28): 26204 – 26210.

63. Carsten R, Christian P, James L, Ulrike S, Rainer HM, Joseph R. Oligomers of the Arginine-rich motif of the HIV –1 TAT protein are capable of transferring plasmid DNA into cells. *J Biol Chem ,* 2002, **278**(13):11411 – 11418.

64. Vendeville A, Rayne F, Bonhoure A, Bettache N, Montcourrier P and Beaumelle B. HIV-1 Tat enters T cells using coated pits before translocation from acidified endosomes and eliciting biological response, *Mol Biol Cell*, 2004, **15**(5): 2347-60.

65. Aldo F, Vittorio P, Caterina A, Antonio F, Mauro G, Fabio B. Caveolae mediated internalization of extracellular HIV – 1 Tat fusion proteins visualized in real time. *Molecular Therapy*, 2003, **8** (2): 284 – 294.

66. Albinsson B, Kidd AH. Adenovirus type 41 lacks an RGD alpha(v)-integrin binding motif on the penton base and undergoes delayed uptake in A549 cells, *Virus Res,* 1999, **64**(2): 125-36.

67. Uduehi A, Mailhos C, Truman H, Thrasher AJ, Kinnon C, Hart SL. Enhancement of integrin-mediated transfection of haematopoietic cells with a synthetic vector system, *Bitechnol Appl Biochem,* 2003, **38**: 201-209.

68. Holcomb IN, Kabakoff RC, Chan B, Baker TW, Gurney A, Henzel W, Nelson C, Lowman HB, Wright BD, Skelton NJ, Frantz GD, Tumas DB, Peale,Jr FV, Shelton DL, Hebert CC. FIZZ1, a novel cysteine-rich secreted protein associated with pulmonary inflammation, defines a new gene family, *The EMBO J,* 2000, **19**(15): 4046-4055.

69. Liu T, Dhanasekaran SM, Jin H, Hu B, Tomlins SA, Chinnaiyan AM, and Phan SH. FIZZ1 stimulation of myofibroblast differentiation, *Am J Pathol*, 2004, **164**(4): 1315:1326.

70. Steppan CM, Bailey ST, Bhat S, Brown EJ, Banerjee RR, Wright CM, Patel HR, Ahima RS and Lazar MA. The hormone resistin links obesity to diabetes, *Nature*, 2001, **409**: 307-312.

71. Yang RZ, Huang Q, Xu A, Mc Lenithan JC, Eison JA, Shuldiner AR, Alkan S and Gong DW. Comparative studies of resistin expression and phylogenomics in human and mouse, *Biochem Biophys Res Commun*, 2003, **310**: 927-935.

72. Teng X, Li D, Champion HC, Johns RA. FIZZ1/RELMα, a novel hypoxia-induced mitogenic factor in lung with vasoconstructive and angiogenicpropertirs, *CircRes,* 2003, **92**: 1065-1067.

73. Li D, Fernandez LG, Dodd-o J, Langer J, Wang D and Laubach VE. Upregulation of hypoxia-induced mitogenic factor in compensatory lung growth after pneumonectomy, *Am J Respir Cell Mol Biol*, 2005, **32**: 185-191.

74. Rose F, Grimminger F, Appel J, Heller M, Pies V, Weissmann N, Schmidt S, Krick S, Camenisch G, Gassmann M, Seeger W, Haenze J. Hypoxic pulmonary artery fibroblasts trigger proliferation of vascular smooth muscle cells: Role of hypoxia inducible transcription factor, *FASEB J*, 2002, **16**: 1660 – 1661.

75. Sieczkarski SB and Whittaker GR. Dissecting virus entry via endocytosis, *J Gen Virol*, 2002, **83**: 1535-1545.

76. Mann DA and Frankel AD. Endocytosis and targeting of exogenous HIV-1 Tat protein, *EMBO J,* 1991, **10**: 1733-1739.

77. Albinsson B and Kidd A H. Adenovirus type 41 lacks an RGD alpha(v)-integrin binding motif on the penton base and undergoes delayed uptake in A549 cells, *Virus Res*, 1999, **64**(2): 125-36.

78. Pelkmans L, Puntener D and Helenius A. Local actin polymerization and dynamin recruitment in SV40-induced internalization of caveolae, *Science*, 2002, **296**: 535-539.

79. Ikonen E and Parton RG. Caveolins and cellular cholesterol balance, *Traffic,* 2000, **1**: 212- 217.

80. Wacker I, Kaether C, Kromer A, Migala A, Almers W and Gerders HH. Microtubule dependent transport of secretory vesicles visualized in real time with a GFP-tagged secretory protein, *J Cell Sci*, 1997, **110**: 1453-1463.

81. Thomsen P, Roepstorff K, Stahlhut M and van Deurs B. Caveolae are highly immobile plasma membrane microdomains, which are not involved in constitutive endocytic trafficking, *Mol Biol Cell,* 2002, **13**: 238-250.

82. Fittipaldi A, Ferrari A, Zoppe M, Arcangeli C, Pellegrini V, Beltram F and Giacca M. Cell membrane lipid rafts mediate caveolar endocytosis of HIV-1 Tat fusion protein, *J Biol Chem,* 2003, **278**(36): 34141-9.

83. Gert HH, Jens P, Lise-Lotte NC, Lissi I and Danielsen EM. Deep-apical tubules: dynamic lipid-raft microdomains in the brush-border region of enterocytes, *Biochem J,* 2003, **373**: 125–132.

84. Frankel AD and Pabo CO. Cellular uptake of the tat protein from human immunodeficiency virus, *Cell,* 1998, **55**(6): 1189-1193.

85. Campbell SM, Crowe SM and Mark J. Lipid rafts and HIV-1: from viral entry to assembly of progeny virions, *J Clin Virol*, 2001, **22**: 217-227.

86. Wagner, K. F., Hellberg, A. K., Balenger, S., Depping, R., Dodd, O. J., Johns, R. A., and Li, D. Hypoxia-induced mitogenic factor has antiapoptotic action and is upregulated in the developing lung: coexpression with hypoxia-inducible factor-2alpha. *Am J Respir Cell Mol Biol,* 2004, **31**: 276-282

87. Steppan, C. M., Brown, E. J., Wright, C. M., Bhat, S., Banerjee, R. R., Dai, C. Y., Enders, G. H., Silberg, D. G., Wen, X., Wu, G. D., and Lazar, M. A. A family of tissue-specific resistin-like molecules. *Proc Natl Acad Sci U S A,* 2001, **98**: 502-506

88. Rajala, M. W., Obici, S., Scherer, P. E., and Rossetti, L. Adipose-derived resistin and gut-derived resistin-like molecule-beta selectively impair insulin action on glucose production. *J Clin Invest,* 2003, **111**: 225-230

Erklärung:

Ich erkläre: Ich habe die vorgelegte Dissertation selbständig, ohne unerlaubte fremde Hilfe und nur mit den Hilfen angefertigt, die ich in der Dissertation angegeben habe. Alle Textstellen, die wörtlich oder sinngemäß aus veröffentlichten oder nicht veröffentlichten Schriften entnommen sind, und alle Angaben, die auf mündlichen Auskünften beruhen, sind als solche kenntlich gemacht. Bei den von mir durchgeführten und in der Dissertation erwähnten Untersuchungen habe ich die Grundsätze guter wissenschaftlicher Praxis, wie sie in der Satzung der Justus-Liebig-Universität Gießen zur Sicherung guter wissenschaftlicher Praxis niedergelegt sind, eingehalten.

Acknowledgements:

Firstly, I would like to extend my sincere thanks to ***Prof. Dr. Werner Seeger***, Department of Internal medicine-2, Der Justus Liebig Universität Gießen, for giving me the opportunity to carry out the study on Non-viral gene transfer in lung cells and its application in pulmonary remodeling studies and for his valuable suggestions.

I thank ***PD. Dr. Jörg Hänze*** for steering me through the project. I would like to thank him for his expert help in designing the experiments, constructive comments, constant concern and support.

I thank ***Prof. Dr. H. M. Piper*** and ***PD. Dr. T. Noll*** for enrolling me in GK 534: ''Biologische grundlagen der vaskulären medizin.'' Their constructive suggestions and constant guidance through out the course of study is highly accoladed.

I thank **Dr. M. Krause**, for constructing the TatRGD peptide. I thank ***Prof. Dr. T. Kissel*** and ***C. Pakhauser***, for helping me with the data on particle size measurements. I thank ***Dr. P. König*** and ***G. Krasteva*** for helping with the confocal microscopy. I thank ***Prof. Dr. Dr. J. Daut*** and ***M. L. Zuzarte*** for providing membrane specific fluorophores.

I thank ***Christiane Hild*** and ***Anette Tsuchner*** for excellent technical assistance.

I thank all my lab members- ***P. Goyal, S. Li, V. Malec, B. Eul and R.K. Savai*** for being wonderful colleagues.

I take this as an opportunity to thank my dear parents and family members for extending their constant encouragement, love and affection.

I would like to extend my heartfelt thanks to my husband, for his loving patience, constant encouragement and valuable discussions during the course of my study.

The financial assistance from the Deutsche Forschungs Gemeinschaft SFB 547, B9 and GK 534 is acknowledged with gratitude.

Lebenslauf:

Personal Details:

Name	:	Aparna Renigunta
Sex	:	Female
Date of Birth		17/04/1979
Place of Birth	:	Nellore, Andhra Pradesh, India.
Nationality		Indian
Marital Status	:	Married
Current Employment	:	PhD., Student (Doktorandin)
Address for Correspondence	:	Medizinische Klinik II,
		C/O Dr. Jörg Hänze,
		Biochemisches Labor,
		1.0G, Friedrichstr. 24,
		D-35392, Giessen.

Education:

Examination	College/University	Duration	Percentage
PhD.,	Der Justus Liebig University Giessen. GK 534, Biologische Grundlagen der vaskularen Medizin.	2002- 2006	
M.Sc., (Biotechnology)	University of Pune	1999 – 2001	62.3% 3rd rank
B.Sc., (Genetics, Botany, Chemistry)	St.Ann's Degree College for Women, Hyderabad Osmania University	1996 - 1999	89%

Awards / Achievements:

- Gold Medal for best academic performance in Biology: St. Ann's College, Osmania University 1996-1999.

- Qualified All India entrance test for Scholarship from Department of Biotechnology, JNU, India.1999 – 2001

- TOEFL: 273 / 300: Year 2002

- Recipient of Glaxo Smith Kline Stiftung, Germany, for poster presentations at the 49th and 50th Annual Biophysical Society meetings, held at Long beach, California, USA in 2005 and Salt lake city, Utah, USA in 2006.

Projects:

- **Masters (M.Sc.,) Diploma Projects:**
1. mt DNA polymorphism for HV – 1 region of D-loop for random Indian population.

    Summer Training, 8May 2000 – 30June 2000
    Center for DNA Finger printing and Diagnostics, Hyderabad, India. Guide: Dr. G.V. Rao

2. Study of Indian evolution as deciphered by mt DNA studies.

    Regular project
    Guide: Dr. Shama Barnabas, National Chemical Laboratories, Pune
            Dr. Yogesh Sauche, National Center for Cell Sciences, Pune

- **Ph.D., thesis:**
Development of a DNA transfer technique for human lung cells with synthetic peptide Tat-RGD and its application for regulatory and functional analysis of RELMβ

    Guide: PD. Dr. Jörg Hänze.
    Dept of Internal Medicine 2, Klinikstr.36, Justus-Liebig-University, 35392-Giessen.

Abstracts / **Conferences:**

- *Analysis of DNA transfection and its improvement with TAT-RGD in lung cells.* EuroSciCon: Efficient transfection of cells, London,UK. (June 2004)

- Deutsche Physiologische Gesellschaft Congress 2004. Leipzig, Germany (2004)

- *Improvement in DNA transfection efficiency in mammalian lung cells with synthetic peptide conjugate TAT-RGD.* Biophysical society 49th annual meeting, Long Beach, California, USA. (12-16,Feb,2005)

- *Human RELMß is a mitogenic factor in lung cells and induced in hypoxia.* Biophysical society 50th annual meeting, Salt Lake City, UT, USA. (18-22, Feb, 2006)

Relevant Publications:

1. Rajkumar Savai, Ralph T. Schermuly, Robert Voswinckel, **Aparna Renigunta**, Bastian Eul, Friedrich Grimminger, Werner Seeger, Frank Rose, and Jörg Hänze. HIF-1α attenuates tumor growth in spite of augmented vascularization in an A549 cell mice tumor model. *Int J Oncol*, 2005 Aug; 27(2): 393-400.

2. **Aparna Renigunta**, Gabriela Krasteva, Peter König, Frank Rose, Walter Klepetko, Friedrich Grimminger, Werner Seeger and Jörg Hänze. DNA transfer into human lung cells is improved with Tat-RGD peptide by caveoli-mediated endocytosis. *Bioconjug Chem*, 2006 Mar-Apr; 17(2): 327-34.

3. **Aparna Renigunta**, Christiane Hild, Frank Rose, Walter Klepetko, Friedrich Grimminger, Werner Seeger and Jörg Hänze. Human RELMbeta is a mitogenic factor in lung cells and is induced in hypoxia. *FEBS Lett*, 2006 Feb 6; 580(3): 900-3.